The Cuprizone-Induced Experimental Demyelination – A Promising Animal Model for Multiple Sclerosis Type III-IV

Ph.D. Thesis

Péter Ács M.D.

Department of Neurology

Medical School of Pécs

University of Pécs, Hungary

Leader of the project: Prof. Sámuel Komoly M.D., Ph.D., Ds.C.

Leader of the program: Prof. Sámuel Komoly M.D., Ph.D., Ds.C.

Leader of Doctoral School: Prof. Sámuel Komoly M.D., Ph.D., Ds.C.

Pécs, 2012

Abbreviations

4HQ: 4-Hydroxyquinazoline

AIF: apoptosis-inducing factor

APC: Adenomatous polyposis coli

C: control

CC: corpus callosum

CNS: central nervous system

Cup: cuprizone

DAPI: 4’6’-diamidino-2-phenylindole

E: 17-estradiol

EAE: experimental autoimmune encephalomyelitis

ERK1/2: extracellular signal-regulated kinase ½

GFAP: glial fibrillary acidic protein

HPRT: hypoxanthine-guanine phosphoribosyltransferase

Iba1: ionized calcium-binding adaptor molecule 1

IGF-1: insulin-like growth factor-1

IHC: immunohistochemistry

JNK: c-Jun N-terminal kinase

LFB: luxol fast blue

MAG: myelin-associated glycoprotein

MAPK: mitogen-activated protein kinase

MBP: myelin basic protein

MRI: magnetic resonance imaging

MS: multiple sclerosis

P: pprogesterone

PARP: poly(ADP-ribose) polymerase

PDGFa-R: platelet-derived growth factor-alpha

PLP: proteolipoprotein

1 Introduction

1.1 Multiple Sclerosis

1.1.1 General characteristics, etiology and pathogenesis of multiple sclerosis

Multiple sclerosis (MS) is a chronic, inflammatory, demyelinating and neurodegenerative disease of the central nervous system (CNS). It is the most common neurological disorder in young adults in the Western hemisphere, being approximately 2 fold more common in females. The precise worldwide prevalence is hard to estimate. It varies between 20 and 150 per 100,000 [1] depending on the country or specific population with a north-to-south gradient in the northern hemisphere and a south-to-north gradient in the southern hemisphere. Generally, MS is less common in people living around the equator [2], but it is possible that the exact frequency of MS is underestimated in these regions. However, recent studies reported that the latitude gradient is decreasing, and the female-to-male MS ratio is increasing [3]. MS is characterized by a broad spectrum of sensory-motor, cognitive and neuropsychiatric symptoms and appears in several distinct disease courses. The majority of the patients are first diagnosed with relapsing–remitting MS (RRMS), where patients develop alternating episodes of neurological symptoms and recovery. This clinical course can last for many years, but within 25 years close to 90% of RRMS patients enter the secondary-progressive stage (SPMS) with a steady progressive neurological decline. Primary progressive MS (PPMS) affects about 10% of MS patients and characterized by slowly accumulating neurological symptoms without recovery. Progressive-relapsing MS (PRMS), affecting 4-10% of MS patients, is characterized by steadily declining neurological disability associated with acute relapses with or without recovery [4, 5]. Recent reports suggest that different clinical courses of MS might be associated with different pathomechanism [6].

The exact pathomechanism of MS is still not entirely understood. Genetic factors [7] and environmental components [8] both influence the susceptibility. The most

widely accepted hypothesis is that MS reflects a primary T cell-mediated autoimmune reaction against the proteins of the myelin sheet which predominantly affects the white matter. It has been suggested that lesion development in MS is associated with activated CD4 T lymphocytes, particularly with the T helper (TH)-1 and TH-17 subpopulations, that cross the blood-brain barrier, activate residential immune cells (microglia, astroglia) and exert direct cytotoxic effects on oligodendrocytes (O L) and myelin in the CNS. As T and B lymphocytes, plasma cells, and macrophages accumulate, pro-inflammatory cytokines amplify the immune response through recruitment of naive microglia. Accompanied by inflammation, edema, plaque-like demyelination, remyelinating OL loss, remyelination, astrogliosis and axonal degeneration develops over time.

1.1.2 Neuropathological features of MS

1.1.2.1 Demyelination and the heterogeneity of MS lesions

The classical neuropathological alteration in MS is the plaque-like demyelinated lesion. Plaques may occur thorough the whole central nervous system, but the most characteristic locations are the periventricular and juxtacortical white matter, and the optic nerve and tract. Typically a venule can be found in the middle of the plaque, with perivascular mononuclear infiltration. The perivascular infiltration contains lymphocytes, plasma cells and macrophages. A detailed histopathological study by Lucchinetti et al. has highlighted the profound heterogeneity in the pattern of demyelination among MS patients [6, 9]. According to these observations lesions can be divided into four distinct patterns with the common hallmark of myelin destruction and the similarities in the inflammatory reaction (composed mainly of T cells and macrophages). Pattern I and II lesions can be described as macrophage- and antibody mediated demyelinating events, respectively. Pattern I lesions are characterized by T cell- and macrophage dominated inflammation and can be considered as sites of active demyelination. Pattern II lesions are similar to

pattern I, but additionally show deposition of immunoglobulin and activated complement at sites of active myelin destruction. Both lesion types are typically centered by small veins or venules and show sharply demarcated edges. Loss of different myelin proteins, such as myelin associated glycoprotein (MAG), myelin oligodendrocyte protein (MOG), proteo-lipid protein (PLP), or CNPase occurs to the same extent. Pattern III lesions are not centered by veins but preservation of a rim of myelin is frequently observed around an inflamed vessel within the demyelinated plaque. The borders of pattern III lesions are ill-defined. Another major difference compared to pattern I and II is that pattern III lesions are characterized by a preferential loss of MAG. Within these areas, myelin-forming OLs show typical signs of apoptosis (nuclear condensation and fragmentation). A pronounced loss of OLs is characteristic at the active plaque border; while OLs are absent in the inactive center. However, pattern III lesions also contain inflammatory elements, composed mainly of T cells and macrophages/microglia, without deposition of immunoglobulin or complement. Pattern IV lesions are described with significant cell death in the periplaque white matter resembling that of pattern III lesions. These lesions also contain microglia/macrophages and T cells (as pattern I lesions). In summary, pattern III and IV lesions can be characterized by signs of OL dystrophy/apoptosis.

Pattern II is the most frequently observed in MS cases, followed in the order of magnitude by pattern III, pattern I, and pattern IV. Interestingly, pattern III lesions were mainly found in patients with less than 2 months duration of disease before biopsy or autopsy [6].

Besides histological heterogeneity recent studies revealed temporal heterogeneity of MS plaques and proposed a novel hypothesis for lesion formation [10]. Studying new symptomatic lesions in patients who died shortly after the onset of a relapse, extensive OL apoptosis (without caspase 3 activation) was observed. The loss of OLs in discrete, still myelinated tissue regions was associated with microglial activation in the absence of mononuclear cell infiltration. Myelin edema and tissue vacuolization seemed to follow the loss of OLs, and to promote the immigration of activated

lymphocytes. A subsequent analysis confirmed that OL apoptosis is the earliest event in prephagocytic lesions with still intact myelin and without T and B cell infiltration in tissue bordering rapidly expanding MS lesions. Phagocytic lesions include macrophages associated with myelin fragmentation, where the role of innate immune response is to scavenge injured myelin. T and B cells are mainly seen in recently demyelinated areas and this adaptive immune response may be associated with OL regeneration [11]. These observations challenge the generally accepted view of a T lymphocyte-initiated demyelination in MS and point out that OL apoptosis may not only occur in type III lesions [6], but rather represents the earliest stage of lesions underlying MS exacerbation [10, 11]. OL and myelin damage expose CNS antigens that subsequently trigger the immigration of mononuclear cells into the CNS. Interactions between MHC Class II positive antigen presenting cells and TH1 / TH17 lymphocytes as well as immunoglobulins, complement and soluble products of activated mononuclear cells may contribute to the amplification of tissue injury [12]. Alternatively, the appearance of adaptive immune response may be associated with OL repair and regeneration [11]. However, an other concise study by Breij et al [13] acknowledges the temporal heterogeneity of early active and developing lesions, but suggests a homogeneous presentation of established demyelinating lesions.

1.1.2.2 Other neuropathological features of MS

There was a paradigm shift in the past decade concerning the focus of MS as it revealed that acute and chronic demyelinating lesions also show extensive axonal injury with transaction [14, 15] that correlates with T-cell and microglial infiltration. Additionally, disease progression in MS depends on accumulated axon degeneration. In the secondary progressive stage, demyelinated areas

coexist with diffuse axonal and neuronal degeneration, accompanied by the accumulation of hyperphosphorylated and insoluble tau [16].

During disease course lesions grow slowly by radial expansion as focal brain inflammation turns into diffuse parenchymal microglial activation and extensive abnormalities of the normal appearing white matter occur [17]. B cells accumulate in the meninges exerting a focal humoral immune response and intrathecal antibody production and damage near the cortex [18]. Primary progressive MS is characterized by reduced plaque load. The signs of inflammation are less evident in this form of the disease, and lymphoid follicles are absent [19].

Besides demyelination, remyelination occurs in MS as well. Remyelination appears as shadow plaques; is the most active during the acute inflammation and associated with the removal of myelin debris by phagocytosis [20]. Undifferentiated OL precursors surround the lesions and promote the remyelination of naked axons [21]. As the disease progresses, with cycles of demyelination and remyelination the CNS loses its capability for proper tissue repair.

1.2 Animal models of MS

Despite severe efforts, the exact pathomechanism of MS still remains elusive. It is widely accepted, that MS is an inflammatory disease, controlled by T cell-mediated autoimmune reaction against the myelin sheet which predominantly affects the white matter. However, this scheme cannot explain the entire spectrum of lesion formation in MS [10]. Although inflammatory lesions typically appear in plaques within the white matter [6], recent histopathological studies have provided evidence that regions of the grey matter are also massively affected [22]. Additionally, diffuse white matter inflammation occurs in the so-called normal appearing white matter [23]. Besides myelin destruction, within active demyelinating lesions acute axonal injury is frequently observed [24].

Moreover, the pattern of demyelination differs between subgroups of patients, and it is suggested that MS follows, at least to some extent, an individual and heterogeneous course. The above mentioned complex and diverse factors require new approaches to understand the entire pathomechanism and to the management of therapy. As mentioned earlier, the mechanism of MS is largely unknown and despite serious efforts there is no cure for it. However, there are several well-characterized experimental animal models that provide a profound insight into the pathological processes that may cause or influence MS.

Although the cuprizone induced experimental demyelination is in the focus of this study, the different approaches of the pathomechanism of MS require a brief overview on other existing models as well.

1.2.1 Experimental allergic encephalomyelitis, virus and toxin induced demyelination models

Experimental allergic encephalomyelitis (EAE) is one of the most frequently used models that mimics MS pathology and allows a detailed insight into the immunological aspects of this disease. This form of experimental encephalomyelitis displays an acute and/or chronic-relapsing, acquired, inflammatory demyelinating autoimmune disease (for reviews see [25-28]). In active EAE, rodents (most commonly mice, rats or guinea pigs) or non-human primates are injected subcutaneously with a myelin related antigen or peptide (MBP, PLP, MOG, etc). Activated myelin-antigen specific $CD4^+$ T cell clones express adhesion molecules, enzymes, cytokines and chemokines and their receptors inducing the break-down of blood-brain barrier and migrating into the CNS. Antigenic determinants presented by antigen presenting cells (monocytes, macrophages, dendritic cells, B cells, microglia, astrocytes) then recognized by myelin-antigen specific T cells, which undergo continuous activation and exert cytotoxic effects in the CNS. A paralytic disease typically develops affecting predominantly the tail and hind limbs, but sometimes also the fore limbs. Acute monophasic as well as chronic relapsing forms of the model were generated.

EAE has been extensively used to better understand immune-mediated mechanisms of demyelination and neurodegeneration in MS. New drug development for MS usually also involves a preclinical testing in the EAE model.

Theiler's murine encephalomyelitis (TMEV) model is based on virus-induced demyelination. Intracranial infection of susceptible mouse strains with TMEV results in biphasic disease of the CNS, consisting of early acute and late chronic demyelinating phase. The late chronic stage of demyelination in the TMEV infection makes this experimental model highly suitable for studying different aspects of the pathomechanism of MS [29].

The common feature of the so called toxin induced demyelination models is that neurotoxic agents are used to induce the loss of myelin sheath in certain areas in the CNS. Experimental models of demyelination based on the use of toxins have provided a remarkable tool for studying the biology of remyelination. The most frequently used demyelinating agents are lysolecithin, ethidium bromide and the copper chelator cuprizone [30].

1.2.2 The cuprizone induced experimental demyelination

The first experiments using cuprizone as a toxic compound were performed in the late 1960s [31]. Although cuprizone was used as a chelator for copper analysis, it was described that cuprizone administration induced microscopic lesions in the brain accompanied by edema, hydrocephalus, demyelination, and astrogliosis [32]. Blakemore reported first that cuprizone causes OL degeneration [33] and the demyelination of the superior cerebellar peduncle [34]. Primary OL degeneration and selective regional vulnerability of the cuprizone regimen were described by Komoly et al [35, 36].

Cuprizone-induced demyelination model has attracted increasing interest during the last decade since contrary to other models of MS this one provides a highly reproducible system of primary OL apoptosis and secondary demyelination. The administration of the copper chelating agent cuprizone (bis-cyclohexanone

oxaldihydrazone) to mice induces spatially and temporally well defined histopathological alterations in the CNS. The earliest event is the appearance of megamitochondria [37], followed by OL apoptosis. The peak of the apoptotic events is between the 3rd and 10th days [38] of the cuprizone challenge, but apoptotic OLs can be detected during the entire administration, and even during the recovery period 12 weeks post treatment [39]. The exact mechanism of OL apoptosis is not fully understood, and is often debated. However, it is generally accepted that cuprizone induces metabolic disturbances in OLs which leads to apoptosis involving a mitochondrial mechanism. A similar role of the mitochondria has been implicated in OL cell loss in MS as well [40].

The massive OL apoptosis is followed by extensive demyelination. The loss of myelin is preceded and accompanied by a down-regulation of myelin-related proteins with varying kinetics. For example, down-regulation of MAG expression can be seen in a few days after the initiation of cuprizone administration, while complete demyelination of the corpus callosum is usually observed after six weeks of treatment. While demyelination was thought to affect only particular white matter tracts (i.e. corpus callosum, superior cerebellar peduncle) [41], recent studies reveal that other regions, including the hippocampus, putamen, cerebellum and even distinct gray matter areas in the cortex, also undergo demyelination [42].

Another prominent pathological feature associated with OL apoptosis is the invasion of the demyelinated areas by activated microglial cells. These cells originate from residential microglia, but macrophages immigrating from the blood [43] also contribute to the marked numbers of phagocytic cells seen most abundantly around the third week of cuprizone treatment. Beyond the phagocytosis of disrupted myelin sheets, the role of activated macrophages and microglia in the cuprizone model is controversial. These cells may further amplify the cuprizone initiated OL cell death by the production and secretion of pro-inflammatory cytokines [44]. Alternatively, microglia may have a beneficial role by stimulating OL precursor cells and promoting remyelination [41].

If mice return to normal diet after six weeks of cuprizone exposure, demyelination is followed by a spontaneous and complete remyelination driven by the repopulation and maturation of OL progenitor cells [45]. If the cuprizone challenge is prolonged for 12 weeks, the degree of remyelination may be limited or remyelination may even fail to occur [39]. If it occurs, this spontaneous but incomplete remyelination begins between the 4^{th} and 6^{th} weeks of the ongoing cuprizone administration [46].

Histopathological features of the cuprizone-induced demyelination closely resemble those of the Lucchinetti et al - defined type III MS lesions [6]. The most significant similarities include a prominent OL apoptosis and microglial activation in the actively demyelinating lesions, the lesions are not perivenous and their borders are ill defined, and there is an early and profound downregulation of the MAG mRNA level [47]. In addition, the cuprizone model shares common features with the earliest phases of MS lesion development as described by Barnett and Prineas [10] and Henderson et al [11], where first, apoptosis of OLs occurs in regions with intact myelin. As the pathology further evolves, early demyelinating lesions are invaded by scavenging macrophages (innate immune response), which phagocytose and clean up degraded myelin. However, in contrast to either the type III lesions or to the acute (earliest) MS lesions, there are no signs of the involvement of the adaptive immune response in lesions seen in the cuprizone model.

Considering the above histopathological features, the cuprizone model is highly suitable for studying basic mechanisms of acute and chronic demyelination and remyelination, exploring the pathophysiology of OL apoptosis, and testing preclinically new interventions for promoting remyelination and repair in MS lesions.

2 Prevention of cuprizone induced demyelination by promoting remyelination or inhibiting OL apoptosis

2.1 Purpose, hypothesis and background of the studies

The goal of our experiments was to investigate whether targeting the survival of OLs (by promoting remyelination or by inhibiting apoptosis) reduces the demyelination in the cuprizone model.

2.1.1 Effect of 17β-estradiol and progesterone treatment on cuprizone induced demyelination in C57BL/6 mice

2.1.1.1 Background

The positive influence of female gonadal steroid hormones [17b-estradiol (E) and progesterone (P)] on neurodegenerative and neurotoxic processes is widely accepted [48, 49]. In patients with MS E and P plasma levels seem to be inversely related to the severity and progression of MS symptoms. The idea that female sex steroids might be a therapeutic option for MS derive from retrospective studies revealing remission of symptoms during pregnancy, disease exacerbation postpartum, and a decreased incidence rate of MS in multipara when compared with nullipara [50, 51]. Prospective studies support these observations and suggest that hormonal alterations during gestation have a protective effect on the course of MS, in particular during the third trimester when hormone levels are massively elevated [52]. After promising results using 17b-estradiol or estriol for treating EAE, a first clinical trial with about 400 patients revealed a beneficial effect of estriol on the course of disease [53-55]. The potency of P to influence MS symptoms and course is far less investigated, and clinical trials have recently started. This is due to the conflicting results obtained in the EAE model which indicated negative as well as positive effects for P on disease progression [56, 57]. In general, both hormones have anti-inflammatory and anti-apoptotic properties in the CNS and play an active neuroprotective role in diverse pathological animal models including stroke, Parkinson’s, and Alzheimer’s disease [48, 49, 58], thus indicating the potency for MS treatment. Protective hormonal effects in first clinical trials as well as in animal experiments using the EAE model were considered to be

the consequence of immune-modulatory functions of sex steroids [59, 60]. However, patients in progressive disease stages have less autoimmune triggered inflammatory lesions [61]. Consequently, the outcome of trials using immune-modulatory medicaments was disappointingly negative [62].

2.1.1.2 Purpose and hypothesis

The aim of this set of experiments was to determine whether the administration of 17β-estradiol and progesterone either alone or in combination affects the cuprizone induced demyelination. We hypothesized that sexual steroid hormones might have a beneficial role against the cuprizone challenge. In our experiments, we used E and P, administered alone or in combination, to prevent demyelination independent of autoimmune reaction. Besides the determination of the myelin status in the CC using different *in vivo* and *in vitro* techniques, we analyzed functional markers of premature and mature OLs and tested the expression of genes responsible for OL recruitment and regulation.

2.1.2 Effect of poly(ADP-ribose) polymerase inhibition on cuprizone induced demyelination

2.1.2.1 Background

Apoptosis-like depletion of OLs has been described in the earliest MS lesions in pathological subtypes for patterns III and IV, suggesting degenerative processes [6]. According to an alternative hypothesis of MS, OL apoptosis represents the first and earliest stage of all lesions, resulting in primary demyelination that unmasks tissue antigens and consequently causes secondary autoimmune inflammation [10]. Additionally, OL depletion occurs progressively during lesion evolution [63]. Recently, mitochondrial dysfunction has been suggested to play a role in the loss of OLs and axons in MS [40]. Pattern III MS lesions with profound OL apoptosis (pattern III) display a pattern of hypoxia-like tissue injury, which seems to be induced by a dysfunction in complex IV of the respiratory chain [6, 64, 65]. In such MS lesions, OL apoptosis follows a caspase-independent pathway [10, 64]. A mitochondrial aetiology in the cuprizone induced demyelination has long been assumed [66]. Supporting this notion, increased production of reactive oxygen

species and reduced activity of various complexes of the respiratory chain were found in the mitochondria of cuprizone-treated OL cells [44]. Impaired mitochondrial respiratory chain results in excessive production of reactive oxygen species and consequent damage to various cellular components including DNA [67]. The nuclear enzyme PARP functions as a DNA damage sensor and signaling molecule, and forms long branches of ADP-ribose polymers on a number of nuclear target proteins, including PARP itself [68]. Extensive DNA damage triggers overactivation of PARP, eventually resulting in cell dysfunction and death [68]. Additionally, PARP activity is required for the translocation of apoptosis-inducing factor (AIF) from the mitochondria to the nucleus, supporting the hypothesis that nuclear mitochondrial crosstalk dependent on poly(ADP-ribosyl)ation is critical in determining the fate of injured cells [69]. This crosstalk involves a PARP-dependent activation of c-Jun N-terminal kinase (JNK) and the cytoprotective phosphoinositol-3 kinase-Akt pathway [70, 71]. Furthermore, PARP functions as a co-activator in the nuclear factor-κB-mediated transcription, regulating the expression of various pro-inflammatory proteins [72]. PARP-mediated cell death and inflammation have been implicated in the pathogenesis of several central nervous system diseases [73]. Inhibition of PARP activity reduced brain injury in ischaemia reperfusion and excitotoxicity [74, 75]. Furthermore, PARP inhibition attenuates inflammation in EAE, the autoimmune model of MS [76].

2.1.2.2 Hypothesis and the aim of the study

Oligodendrocyte apoptosis is a common feature of cuprizone induced demyelination and certain hystopathological types of MS. In the cuprizone model OL apoptosis is – at least partly – induced by the disruption of mitochondrial respiratory chain and complex IV. This process induces DNA damage of the affected cells. We hypothesized that the mitochondrial impairment and consequent DNA damage is associated with poly(ADP-ribose) polymerase (PARP) overactivation contributing to OL cell loss in the cuprizone challenge.

In this study we aimed to investigate whether a.) PARP overactivation contributes to the OL cell loss in the cuprizone model, whether b.) inhibition of PARP has a

beneficial role in the cuprizone induced demyelination. Additionally, our purpose was to learn if PARP overactivation is present in human MS plaques and plays a role in OL cell death.

2.2 Materials and methods

2.2.1 Animals

C57BL/6 male mice were bred and maintained in a pathogen-free environment. Food and water were available ad libitum. All animal experiments were carried out under legislation [1998/XXVIII Act of the Hungarian Parliament on Animal Protection and Consideration and Decree in Scientific Procedures of Animal Experiments (243/1998)] in laboratories in the University of Pecs. Licensing of procedures was controlled by The Committee on Animal Research of the University of Pecs according to the Ethical Codex of Animal Experiments. Research and animal care procedures were approved by the Review Board for the Care of Animal Subjects of the district government (Nordrhein- Westfalen, Germany).

2.2.2 Experimental designs and groups

2.2.2.1 Administration of estrogen and progesterone

Demyelination was induced by feeding 8-week-old male mice a diet containing 0.2% cuprizone mixed into a ground standard rodent chow for 5 weeks. Animals were treated with progesterone (25 µg per injection), 17b-estradiol (50 ng per injection), or with a mixture of both hormones using subcutaneous depot injections in the neck region twice a week. Preliminary dose-finding studies revealed that the chosen steroid concentrations yielded plasma levels of both steroids of approximately 50 pg/mL (E) and 25 ng/mL (P), respectively. Two injections per week were chosen, because in pilot experiments we observed that a single application per week is accompanied by a gradual decline of steroid plasma levels in the second half of the week down to 20% of originally

applied concentrations. Sex- and age matched vehicle treated animals were used as controls.

Ten mice were used for IHC and eight mice for gene expression analysis in each group, namely placebo, the cuprizone group, cuprizone plus E, cuprizone plus P, and cuprizone plus E/P group. Furthermore, five animals were treated with either E or P or a combination of both hormones for 1 week to serve as hormone-only group without cuprizone. This group was used for gene expression analysis to exclude that gene expression of investigated genes is influenced by the chosen hormonal treatment.

2.2.2.2 Administration of PARP inhibitor

Starting at 8 weeks of age, mice received a diet of powdered rodent chow containing 0.2% cuprizone by weight for 3, 5 and 6 weeks ad libitum to induce demyelination. The PARP inhibitor 4-hydroxyquinazoline (4HQ) [77] was administered i.p. at a dose of 100 mg/kg body mass and a volume of 10 ml/g body mass every day [78], starting on the same day as the cuprizone treatment. Control mice received the same volume (10 ml/g) of saline solution instead of 4HQ.

2.2.3 Tissue preparation

For histological and immunohistochemical studies, mice were intracardially perfused with 4% paraformaldehyde containing picric acid after 5 weeks of cuprizone treatment. After overnight postfixation, brains were dissected. Paraffin-embedded brains were coronally sectioned each 8 µm in thickness at the levels of 161, 181, 209, and 221 according to mouse brain atlas by Sidman et al. (http://www.hms.harvard.edu/research/brain/atlas.html). For gene expression analysis, mice were killed by rapid decapitation. Brains were quickly removed, and the entire CC dissected using a stereo-microscopic approach. Tissues were immediately frozen in liquid nitrogen and kept at -80℃ until used.

2.2.4 Histopathology and scoring of demyelination in cuprizone lesions

Demyelination was evaluated in 8 µm paraffin sections at different levels of the brain using Luxol fast blue (LFB) staining with Cresyl violet. Sections were placed on gelatine-coated slides, deparaffinized, hydrated to 95% alcohol, and incubated in a LFB solution (0.01%) overnight at 60℃. After that, sections were differentiated in a lithium carbonate solution (0.05%) and counterstained with Cresyl-violet (myelinated fibers appear blue, the neuropil pink, and nerve cells purple). To evaluate demyelination in LFB-stained sections, three independent blinded readers scored LFB/cresyl violet-stained sections between zero and three. A score of three is equivalent to the myelin status of a mouse not treated with cuprizone, whereas zero is equivalent to totally demyelinated CC. A score of one or two corresponds to one-third or two-third fiber myelination of the CC, respectively. Ten animals of each group were included in the study.

2.2.5 Immunohistochemistry, immunofluorescence and confocal microscopy of cuprizone lesions

Sections were placed on silan-coated slides, rehydrated and heat-unmasked, then, blocked with a PBS solution containing 2% normal horse, and incubated overnight with the primary antibody diluted in blocking solution. Anti-myelin basic protein antibody (1:75, Novocastra Laboratories), anti-glial fibrillary acidic protein (GFAP, 1:500, DAKO) were used for routine staining procedures. Mature oligodendrocytes were stained using anti-APC (Ab-7) monoclonal antibody (CC-1) (1:200; Calbiochem), whereas anti-Iba1 antibody (1:250, Wako) was used as a macrophage marker. Monoclonal rat anti-mouse Ki-67 Antigen, clone TEC-3 (1:25, DakoCytomation) was used for labeling mitotic cells. For the visualization of PAR and AIF poly(ADP-ribose) (1:100, Alexis Biotechnology) and AIF (1:100, Cell Signalling Technology) antibodies were used respectively. Appropriate biotinylated secondary antibodies were used (1:200, Molecular Probes). For visualization, the ABC Kit (Vector Laboratories) and the DAB reaction were used. Sections were viewed with a BX-50 microscope (Olympus, Germany) and photographed using a SPOT RT color digital system. Immunopositive OLs within

the CC showing a clearly visible nucleus were counted. Cell numbers were calculated and expressed per 0.1 mm^2. Cell counting was performed in two slices of each investigated brain region using an Axiophot microscope (Zeiss, Germany) with a 40x objective.

For immunofluorescent labelling, Alexa 488 goat anti-rabbit secondary antibody (1:200, Molecular Probes) was applied with DAPI counterstaining for visualization of nuclei. Confocal images were collected using an Olympus Fluoview FV-1000 laser scanning confocal imaging system and an Olympus UPLSAPO 60x oil immersion objective lens (numeric aperture 1, 35). Cell nuclei were counterstained with DAPI, the dye was excited at 405 nm and its emission was detected in the range of 425–475 nm. Antibody binding was detected by using Alexa 488 excited with a 488nm laser beam and detected in the range of 500–600 nm. Scanning of images occurred in a sequential line mode using line Kalman integration count 4. The confocal aperture was set to 100 mm. Supplemented images represent areas of 52398x52398 µm at a resolution of 640x640 pixels. With the imaging conditions used, there was no detectable bleedthrough of fluorescence from one channel to the other when we studied single-labeled specimen.

2.2.6 Immunocytochemistry and confocal laser fluorescence microscopy for poly(ADP-ribose) and apoptosis-inducing factor in human MS lesions

Poly(ADP-ribose) and AIF expression was studied in the lesions of 13 patients with MS and 5 control cases without neurological disease or brain lesions. The MS samples contained six cases with acute multiple sclerosis (Marburg, 1906), one case with relapsing remitting multiple sclerosis and six cases with chronic progressive multiple sclerosis (Table 1). Lesion areas within the sections were defined according to activity: early pattern III lesions showed loss of myelin-associated glycoprotein (MAG), OL apoptosis and predominant infiltration by activated microglia; late active/inactive lesions in pattern III MS cases were densely infiltrated by macrophages with a variable content of myelin degradation products; normal appearing white matter areas were at least 1 cm apart from the active lesions. In pattern II lesions, early stages revealed scattered infiltration of

the tissue with macrophages and activated microglia; myelin sheaths were still present, but showed signs of acute dissolution. In late active/inactive pattern II lesions, myelin was completely lost and macrophages contained myelin degradation products at various stages of chemical myelin disintegration. The lesions in patients with progressive MS were slowly expanding lesions with a small rim of active demyelination (early lesions) with microglia activation and some macrophages containing the earliest stages of myelin degradation. The late active/inactive lesion centers were completely demyelinated and contained a variable, but generally low amount of macrophages with myelin degradation products. Active lesions following pattern III [6] were seen in four cases with acute MS, pattern II lesions were analyzed in two cases of acute MS and one case with relapsing–remitting MS, and slowly expanding active lesions were present in six cases with progressive MS [17]. Immunocytochemistry was performed on paraffin sections [79] without antigen retrieval. Poly(ADP-ribose) antibody was purchased from Alexis Biotechnology, and the AIF antibody from Chemikon International. For lesion characterization we used immunocytochemistry with antibodies against MAG, myelin oligodendrocyte glycoprotein, proteolipid protein, cyclic nucleotide phosphodiesterase and CD68. Fluorescence immunohistochemistry was performed on paraffin sections [80]. Staining with primary antibody poly(ADP-ribose) or AIF was done overnight. As a second step, sections were incubated with a secondary biotinylated-anti-mouse antibody (Amersham Pharmacia Biotech; 1:200). This was followed by antigen retrieval by 60 min incubation in a plastic coplin jar filled with citrate buffer (0.01 M, pH 6.0) in a household food steamer device. This first staining was finished with application of streptavidin-Cy2 (Jackson ImmunoResearch, 1:75) for 1 h at room temperature. After washing in tris-buffered saline, the sections were incubated overnight with anti-carbonic anhydrase II (The Binding Site Ltd, Birmingham, UK, for detection of oligodendrocytes). This was followed by washing and incubation with secondary Cy3-conjugated antibodies donkey anti-sheep or donkey-anti-rabbit (both 1:100, both Jackson Immuno Research). The staining was finished with DAPI counter stain. Sections were examined using a

confocal laser scan microscope (Leica SP5, Mannheim, Germany). Recordings for Cy2 (excited with the 488nm laser) and Cy3 (excited with the 543nm laser) were done simultaneously and followed by recording for DAPI with a 405nm laser.

For quantification of AIF expression only those cells were counted that showed unequivocal immunoreactivity within their nuclei. Cells were counted manually in each of the above-defined areas in seven microscopic fields of 0.27mm^2 each. The values given in Table 3 represent cells/mm^2.

Table 1. Clinical data for multiple sclerosis patients

Table 2						
Case	Multiple sclerosis type	Gender	Age (years)	Duration (months)	Initial/early	Late act/inactive
MS III A	AcMS	Male	45	0.2	2	1
MS III B	AcMS	Male	45	0.6	3	2
MS III C	AcMS	Male	35	1.5	5	4
MS III D	AcMS	Male	78	2	1	1
MS II A	AcMS	Male	52	1.5	4	4
MS II B	AcMS	Female	51	5	2	1
MS II C	RRMS	Female	57	156	2	3
Chr MS A	SPMS	Male	41	137	2(SEL)	2
Chr MS B	SPMS	Male	56	372	1(SEL)	2
Chr MS C	SPMS	Female	46	444	2(SEL)	2
Chr MS D	PPMS	Male	67	87	1(SEL)	1
Chr MS E	PPMS	Female	77	168	1(SEL)	1
Chr MS F	PPMS	Female	71	264	2(SEL)	3
Normal controls		3 Males / 2 Females	36-74		0	0

MS III = multiple sclerosis patients with pattern III lesions; MS II = multiple sclerosis cases with pattern II lesions; Chr MS= multiple sclerosis cases with slowly expanding lesions of progressive multiple sclerosis;
AcMS = acute multiple sclerosis; RRMS = relapsing/remitting multiple sclerosis; SPMS = secondary progressive multiple sclerosis; PPMS = primary progressive multiple sclerosis;
Initial/early = lesions at the early active stage of demyelination (in pattern III lesions in areas of MAG loss); Late act/inactive = late active or inactive lesions, still containing macrophages with degradation products of different stages of myelin digestion;
SEL = slowly expanding lesions with a small rim of microglia activation and early myelin degradation products at the margin.
The numbers in the last two columns represent the numbers of different lesion types contained in the sections.

2.2.7 MRI

Mice were anesthetized by intraperitoneal injection of diazepam (5 mg/kg) and ketamine (80 mg/kg). Animals were fixed into an epoxy resin animal holder tube modified to accommodate the tip of teeth and position the eyes of each animal to the same location: 5.0 ± 0.5 mm above the isocenter of the magnet. A glass capillary, filled with water and glycerol in a 9:1 mixture, was placed near the head of the animal for external signal intensity reference. MR images were obtained using a Varian INOVA 400 WB NMR spectrometer with an 89-mm vertical bore magnet of 9.4 T using a 35-mm inner diameter hollow microimaging probe with a Litz-type transmit/receive volume RF coil and built-in self-shielded water-cooled gradient system with 600 mT/m gradient strength and <100 µm rise time. Postprocessing was performed by VNMR 6.1C and Image Browser software on a Sun Ultra 30 workstation.

2.2.8 Quantitative RT-PCR (qPCR)

For gene expression analysis, mice were killed by rapid decapitation. Brains were quickly removed, corpus callosum was dissected and immediately frozen in liquid nitrogen, and kept at -70℃ until used. Isol ation of total RNA was performed with NucleoSpin kit (Macherey-Nagel). RNA concentration and purity were assessed using OD260 and OD260/OD280 ratio, respectively, and reverse transcribed using an Invitrogen M-MLV RT-kit and random hexanucleotide primers. Gene expression was measured using the qPCR technology (BioRad), QTM SYBR Green Supermix (BioRad), and a standardized protocol. Primer sequences are shown in Table 2. Relative quantification was performed using the ΔCT method. Hypoxanthine-guanine phosphoribosyltransferase (HPRT) was used as a housekeeping reference gene. Data were expressed as the ratio of the amount each transcript versus the concentration of HPRT. Melting curves and gel electrophoresis of the PCR products were routinely performed to determine the specificity of the PCR reaction.

Table 2. Primer sequences for qPCR experiments

Table 1			
Gene	Sense	Antisense	bp Length
MBP	cca tcc aag aag acc cca ca	ccc ctg tca ccg cta aag aa	191
PLP	tgg cga cta caa gac cac ca	gac aca ccc gct cca aag aa	115
GFAP	gag atg atg gag ctc aat gac c	ctg gat ctc ctc ctc cag cga	380
PDGFaR	tca aga gag agg acg aga cc	gca aga ggc aac acg gat aa	287
IGF-1	cta cca aaa tga ccg cac ct	cac gaa ctg aag agc atc ca	154
HPRT	gct ggt gaa aaggac ctc t	cac agg act aga aca cct gc	248

2.2.9 Immunoblot analysis

Tissue samples were taken from animals killed after 3 or 5 weeks of treatment. Corpora callosi of the mice were carefully dissected and 25 mg of the tissue was homogenized in ice-cold 10mM tris buffer, pH 7.4 [containing 0.5mM sodium metavanadate, 1mM ethylenediaminetetraacetic acid and protease inhibitor cocktail (1:200); all purchased from Sigma]. Homogenates (10 mg each) were loaded onto 10 and 12% sodium dodecyl sulphate polyacrylamide gels, electrophoresed and transferred to nitrocellulose membranes. The following antibodies were used: anti-MBP (1:1000) (Novocastra Laboratories Ltd), anti-poly(ADP-ribose) (1:1000) (Alexis Biotechnology), anti-AIF (1:300) (Santa Cruz Biotechnology), anti-phospho-Akt (Ser473) (1:1000) (R&D Systems), anti-caspase-3 (1:1000), anti-nonphosphorylated Akt/protein kinase B (1:1000), anti-extracellular signal-regulated kinase ½ (ERK1/2) (Thr183/Tyr185) (1:1000), anti-phospho JNK (Thr183/Tyr185) (1:1000), anti-caspase-3 (1:1000) (all from Cell Signalling Technology), anti-phospho-p38-mitogen-activated protein kinase (MAPK) (Thr180/Tyr182) (1:1000) and anti-actin (1:10 000) (both from Sigma). Appropriate horseradish peroxidase-conjugated secondary antibodies were used at a 1:5000 dilution (anti-mouse and anti-rabbit IgGs; Sigma) and visualized by enhanced chemiluminescence (Amersham Biosciences). Films were scanned and the pixel volumes of the bands were determined using National Institutes of Health Image J software.

2.2.10 Caspase-3 activity assay

Carefully dissected corpus callosum samples (20 mg) from animals treated for 3 weeks were homogenized in the lysis buffer (50mM Tris, pH 8) containing protease inhibitor cocktail (Sigma). Fluorometric assays were performed using fluorescent-labeled peptide substrate for caspase-3 (Ac-DEVD-AFC, Sigma) and a fluorescence plate reader set at 360nm excitation and 460nm emission, as recommended by the manufacturer.

2.2.11 Statistical analysis

For the quantitative analysis of mature oligodendrocytes and mitotic cells in the hormone administration study, APC-immunopositive or KI67-immunopositive cells, respectively, were counted manually of 10 E/P-treated, 10 cuprizone-treated, and 10 control mice at the level of section 221 (Sidman et al., see Materials). Raw scores were calculated per 0.1 mm^2. Three sections per animal were analyzed for scoring. Image processing, analysis, and measurements were carried out using NIH Image J software. Determination of demyelination in LFB stained sections was performed in 10 animals of each group. The degree of myelination between different experimental groups was compared using the Mann-Whitney rank test for scoring results. For OL cell counting, one-way ANOVA test was used. Scheffe post-hoc test was applied for detecting differences between groups. For gene expression analysis, statistics were made using the rough data of all experiments. Eight animals of each group were included in the study. Differences between groups were statistically tested by analysis of variance (ANOVA) followed by Tukeys's post-hoc multiple-range test using SPSS software. The density of poly(ADP-ribose) and AIF-positive cells (Table 3) in each group of MS patients was compared with the respective values found in normal white matter of control brains using Scheffe´'s post hoc ANOVA test; heteroscedasticity was minimized with the logarithmic transformation. The immunoblot band intensities were normalized to the loading control and compared pair wise using Scheffe´'s post hoc ANOVA test; heteroscedasticity

was minimized with the logarithmic transformation. Differences were considered significant at values of $P < 0.05$ or lower.

2.3 Results

2.3.1 Effect of 17β-estradiol and progesterone treatment on cuprizone induced demyelination in C57BL6 mice

2.3.1.1 Effect of hormone treatment on the cuprizone induced demyelination and mature OL loss

In the cuprizone treated group *in vivo* T2 weighted MRI images revealed increased signal intensity within the CC indicating massive demyelination (Fig. 1). Additionally, T2-weighted images also showed an increase in ventricle volumes in the cuprizone group pointing at a manifested hydrocephalus. The appearance of a hydrocephalus is a well-known phenomenon in the cuprizone model [38]. The administration of E and P significantly reduced CC demyelination in T2-weighted MR images and diminished ventricle swelling (Fig. 1). To confirm the results obtained by MRI, LFB staining was performed and the myelin score was determined in the experimental groups. Cuprizone feeding resulted in a profound and significant demyelination of the CC as shown in Fig. 1. The administration of E and P significantly reduced CC demyelination as demonstrated by LFB staining (Fig. 1). Quantification of myelin scores (LFB) revealed that cuprizone significantly impaired the myelin score to 1 when compared with controls (Score 3). Single applications of E or P only moderately abolished this negative effect (data not shown). The administration of both hormones, however, returned myelin score to >2 (Fig. 1). Data always showed intermediate responses of single hormone application versus significantly better myelination score after coapplication of the hormones. For further quantification, gene expression of MBP (Fig. 1) and PLP (data not shown), both markers for mature myelin synthesizing OLs, were analyzed by rtPCR. As indicated in Fig 1, cuprizone exposure led to a highly significant down-regulation of both myelin markers. The application of E and P caused a significant up-regulation of MBP and PLP, although it appears less obvious than myelin scores of the same animals would suggest. Levels were only restored to approximately 45% and 30% of controls for MBP and PLP, respectively. Single steroid hormones had almost no effect on both parameters. Immunostaining for APC to label mature

OLs within the CC showed a massive decline (>60%) in the number of APC-positive cells after the cuprizone challenge (Fig. 1) which was significantly antagonized by both steroid hormones. Moreover, after E/P treatment, the number and distribution OLs were comparable with the control group (Fig. 1).

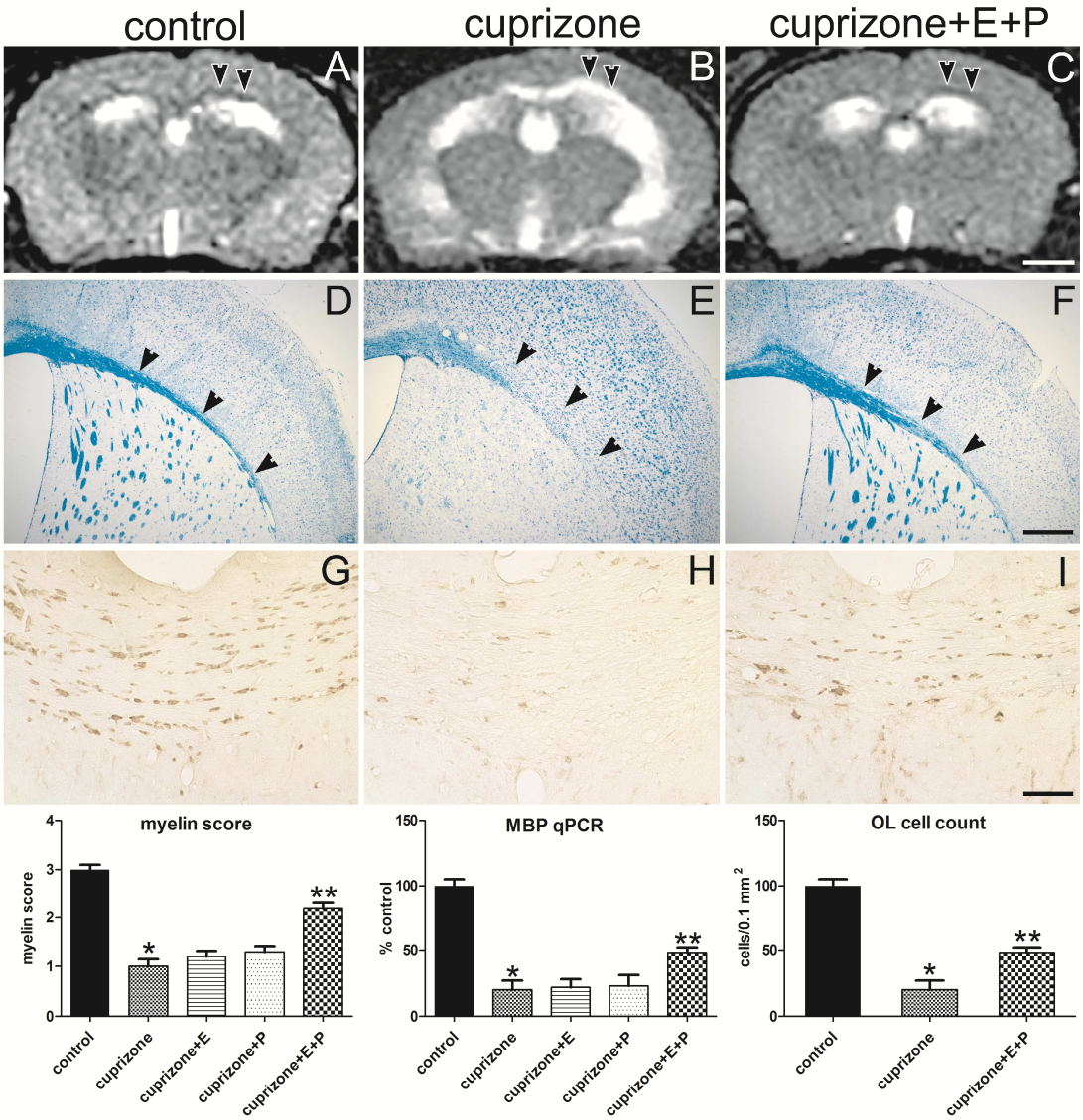

Figure 1. Effect of cuprizone and estrogen (E) plus progesterone (P) administration on myelination of the corpus callosum in mice. **A-C:** Representative T2 weighted MRI images of control (A), cuprizone treated (B) and cuprizone plus E and P treated mice. Note that the corpus callosum (indicated by black arrows) is hyperintense in the cuprizone treated mice indicating demyelination, while this effect was abolished by E and P (C). Scale bar: 1 mm. **D-F:** LFB staining shows profound demyelination in the corpus callosum (black arrows) in cuprizone treated mice (E). The myelination is intact in the E and P treated mice (F). Scale bar: 0.5 mm. **G-I:** APC immunohystochemistry to visualize mature oligodendrocytes (OL) in the midline of the corpus callosum. Note that the cuprizone treatment induced an almost total loss of mature OLs (H), while the number and arrangement of OLs in the E and P treated mice (I) is comparable with the control mice (G). Scale bar: 100 µm. **Lower panel:** quantitative evaluation of the demyelination and OL loss by determination of the myelin score (graph on the left), MBP qPCR (middle) and OL cell count (graph on the right). For details see text. * indicates $p<0.001$ cuprizone vs. control, ** indicates $p<0.01$ cuprizone plus E/P vs. cuprizone.

2.3.1.2 Macrophage infiltration and astrocyte reaction in the experimental groups

Because the modulation of astroglial or microglial function might be associated with the myelin restoration, we analyzed the effect of E and P on the presence/absence of these cell types in the demyelinated CC using immunohistochemistry for GFAP and Iba1, a pan macrophage marker. In addition, GFAP mRNA expression was quantified by qPCR (data not shown). We observed a pronounced astrocytosis in cuprizone-fed animals (Fig. 2). Interestingly, this effect was multiplied after the application of E and P (Fig. 2). Expression analysis confirmed these data and revealed an approximately 12-and 18-fold increase in GFAP mRNA levels in cup- and cup-plus E/P-treated mice, respectively, when compared with controls. Single administration of E or P together with the cup did not show a significant up-regulation of GFAP mRNA expression (data not shown). Macrophage invasion demonstrated by the presence of Iba1-positive cells was seen in the lateral part of the CC in cuprizone-fed mice (Fig 2.). In E/P-treated animals, macrophage infiltration was not only observed in the lateral part but additionally in the midline of CC (Fig. 2).

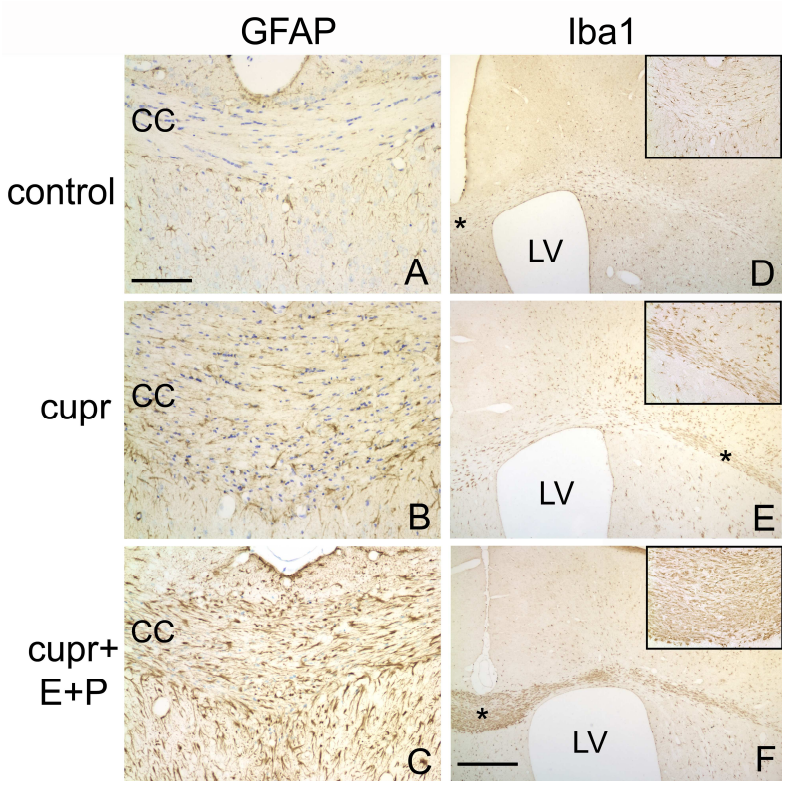

Figure 2. Effect of cuprizone (cupr) and estrogen (E)/progesterone (P) treatment on the number of GFAP-positive astrocytes (A-C) and Iba-1-positive macrophages/microglia (D-F) in the corpus callosum (CC). Cuprizone increased the number of astrocytes in the midline of the CC (B). Note that in cuprizone plus E/P-treated mice (C), astrocytosis is stronger than in cuprizone-exposed CC. In control animals, only few Iba-1-positive macrophages/microglia are visible in the medial and lateral part of the CC (D). In response to the cuprizone challenge, the lateral part of the CC is infiltrated by macrophages (E). After hormonal treatment, almost the entire CC (including the midline) is infiltrated by macrophages (F). Asterisks in D-F indicate the areas which are shown as inserts and at higher magnification. Scale bar represents 100 µm in A and 500 µm in F.

2.3.1.3 Expression of OL maturation-related genes in the cuprizone and hormone treated mice

Protective hormonal effects on myelination status in the CC may be the consequence of the recruitment of oligodendrocyte progenitors which account for new myelin sheets. To follow this hypothesis, we have analyzed expression levels of platelet-derived growth factor alpha receptor (PDGFα-R) in the CC, a stringent marker of premature oligodendrocytes. PDGFα-R mRNA levels displayed a tendency to be higher in cup-fed animals when compared with controls (c 100 ± 3 vs. cup 122 ± 11) without reaching statistically significant values (Fig. 3). In contrast, mRNA levels were significantly higher in the cup+E/P group when compared with controls (c 100 ± 3 vs. cup+E/P 145 ± 20, $P < 0.05$) (Fig. 3) implicating proliferation of premature oligodendrocytes in response to hormonal treatment. This is strongly supported by immunohistochemistry for Ki-67, a marker for cell proliferation, in the CC. Only few Ki-67-positive cells were found in controls and after cup-treatment in the sub-ventricular zone and in the lateral part of the CC, whereas numerous Ki-67 positive cells were detected in all parts of the CC after E/P treatment (Fig 3). Insulin-like growth factor-1 (IGF-1) is a well-known mitogen for premature OLs, and astrocytes the major sources for brain IGF-1 synthesis [36, 81]. As we observed a massive astrogliosis within the CC, we studied gene expression of IGF-1 in the CC. IGF-1 mRNA levels were significantly increased by approximately 20-fold in cup-fed mice when compared with controls and by more than 40-fold in cup+E/P-treated animals (Fig. 3). Similar to the regulation of GFAP expression, the application of single hormones together with cup did not significantly stimulate IGF-1 mRNA expression (data not shown).

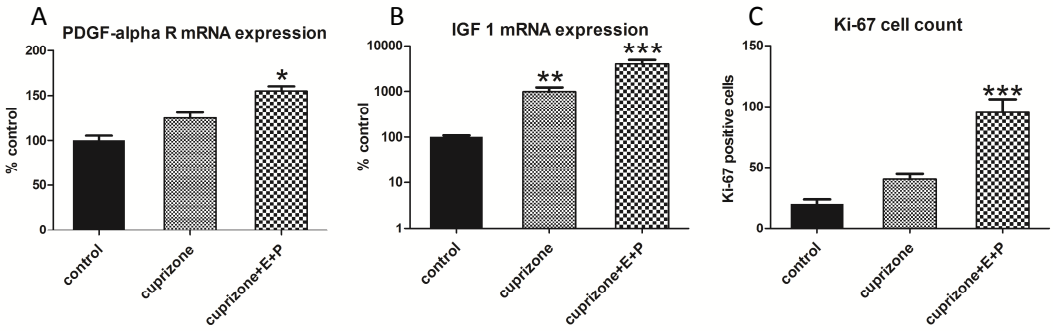

Figure 3. Expression of remyelination-related genes, and the number of Ki-67 positive cells in the corpus callosum. **A:** PDGF-alpha R expression in the corpus callosum. Note that only cuprizone plus estrogen/progesterone (E+P) administration increased significantly the PDGF-alpha R expression. *p < 0.05 control vs. cup + E/P. **B:** IGF-1 expression was massively induced by cuprizone, as well as by cuprizone plus E+P treatment. **p < 0.001 control vs. cup, ***p < 0.0001 cup vs. cup + E/P in B. **C** demonstates the number of Ki-67-positive cells. ***P < 0.05 E+P plus cuprizone vs. cuprizone.

2.3.2 Effect of poly(ADP-ribose) polymerase inhibition on cuprizone induced demyelination

2.3.2.1 Cuprizone enhances PARP activation in the corpus callosum

To investigate the effect of PARP inhibition on experimental demyelination, we first examined the activation of PARP upon cuprizone treatment. Cuprizone induced auto-poly(ADP-ribosyl)-ation, i.e. activation of PARP in the CC of mice after 3 weeks of treatment (Fig. 4). Expression of poly(ADP-ribose) immunoreactivity in the apoptotic nuclei of oligodendrocytes was confirmed by confocal laser microscopy (Fig. 4). In addition, 4HQ - a potent inhibitor of the enzyme - blocked both cuprizone induced and basal auto-poly(ADP-ribosyl)ation at a dose of 100 mg/kg used throughout this study (Fig. 4). This dose of 4HQ was previously found to be effective and devoid of any apparent toxic effect [78].

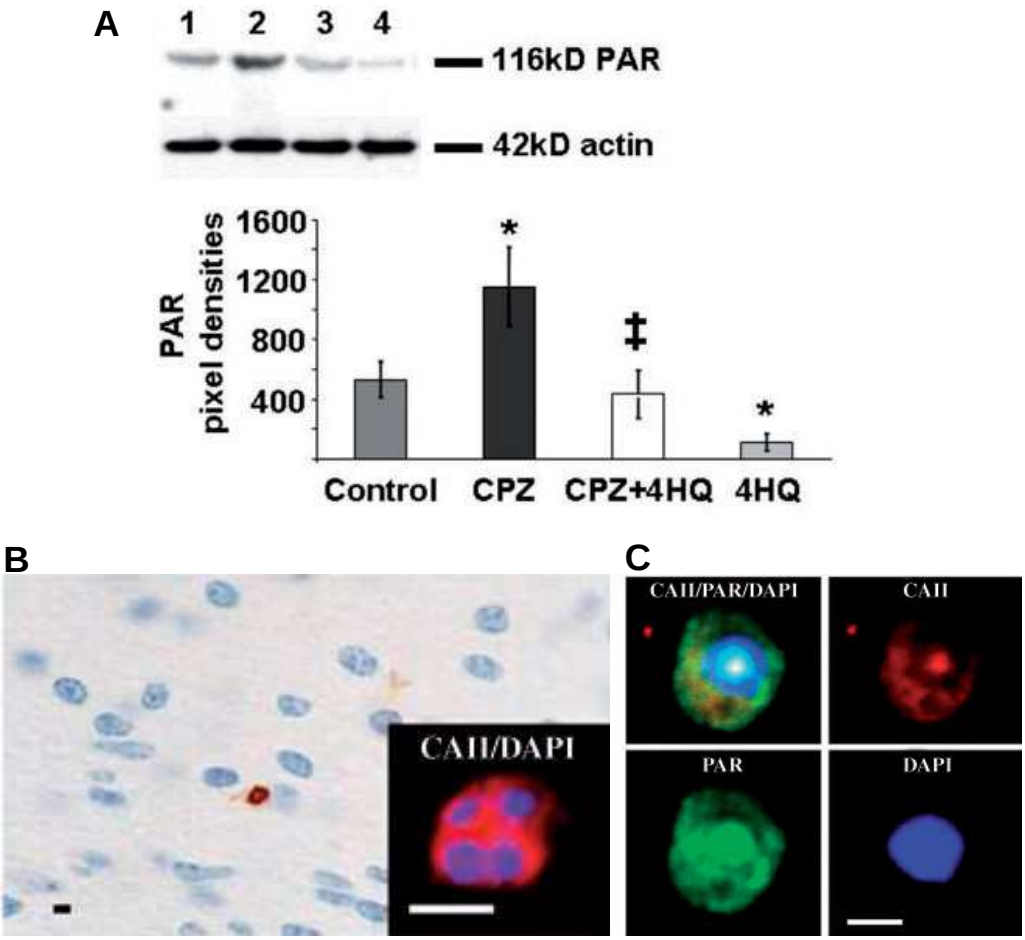

Figure 4. Effect of cuprizone and 4HQ treatment on poly(ADP-ribose) polymerase activation.

A: Representative immunoblots for PARP auto-ADP-ribosylation (upper panel) and their densitometric evaluation (lower panel) in the corpus callosum of mice treated for 3 weeks. Lane 1 = control; lane 2 = cuprizone treatment (CPZ); lane 3 = cuprizone and 4HQ (CPZ and 4HQ) treatment; lane 4 =4HQ only. Results on the diagram are expressed as mean pixel densities ±SD; * $p<0.05$ compared with control; ‡$p<0.05$ compared with cuprizone group.

B: Representative anti-poly(ADP-ribose) (PAR) immunohistochemistry of the corpus callosum in a cuprizone-treated mouse. Brown color indicates strong poly(ADP-ribose) reactivity in the nucleus of an oligodendrocyte with condensed nuclei in active lesion. The insert indicates an apoptotic oligodendrocyte stained for carboanhydrase II as a marker for oligodendrocytes and DAPI, showing the fragmented nucleus (scale bar: 10 µm).

C: Representative confocal images of PARP activation in an oligodendrocyte. Carbonic anhydrase II immunoreactivity (red), poly(ADP-ribose) immunoreactivity (green) and DAPI nuclear staining (blue) were presented individually and merged (left upper panel) (scale bar: 10 µm).

2.3.2.2 PARP inhibition protects against cuprizone induced demyelination

Examination of the brain was performed by non-invasive *in vivo* MRI. In untreated mice, CC appeared hypointense on T2-weighted images (Fig. 5). Upon cuprizone feeding, T2-weighted images of the CC showed hyperintensity corresponding to demyelination, that was most pronounced after 4 weeks. PARP inhibitor prevented cuprizone-induced hyperintensities in the CC (Fig. 5). Inhibition of PARP prevented demyelination. When applied alone, 4HQ did not cause any changes in signal intensities (Fig. 5). Pathological analysis with LFB-cresyl violet staining revealed a profound demyelination in the CC of cuprizone-fed mice (Fig. 5). According to a semi-quantitative histological analysis, 4HQ reduced the cuprizone-induced demyelination ($P<0.001$) (data not shown). 4HQ alone did not affect myelination. Quantitative MBP immunoblotting revealed decreased MBP expression after 5 weeks of cuprizone feeding ($P<0.01$), which was reversed by the PARP inhibitor 4HQ ($P<0.05$). The administration of the PARP inhibitor alone did not affect the MBP level (Fig. 5). Similar results were found by MBP immunohistochemistry (data not shown).

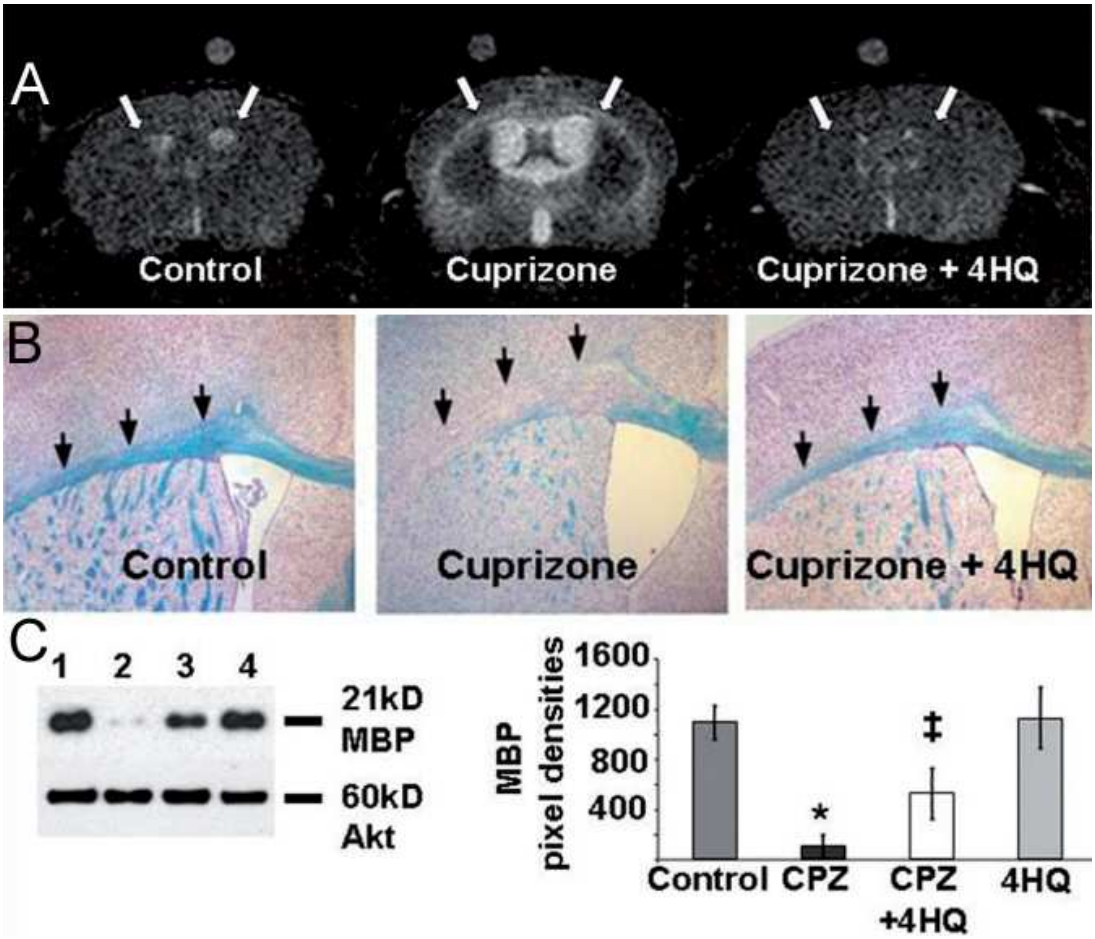

Figure 5. Effect of cuprizone and 4HQ treatment on demyelination in the corpus callosum.

A. Representative T2-weighted MRI images of brain coronal sections of mice treated for 4 weeks. Arrows indicate hyperintensities (suggesting demyelination) or hypointensity (intact myelin status) in the corpus callosum.

B. Representative Luxol fast blue images in the corpus callosum (arrows) on coronal brain sections of mice treated for 5 weeks. Blue staining indicates intact myelin sheath.

C. MBP expression in the dissected corpus callosum of mice treated for 5 weeks was detected by immunoblotting utilizing an anti-MBP antibody. Even protein loadings were confirmed by an anti-Akt antibody and immunoblotting. Representative immunoblots (left panel) from three experiments with similar results and densitometric evaluation (right panel) are shown. Lane 1 = control; lane 2 = cuprizone (CPZ) treatment; lane 3 = cuprizone+4HQ (CPZ+4HQ) treatment; lane 4 =4HQ only. Results on the diagram are expressed as the mean pixel densities ±SD; *$p<0.01$ compared with control; ǂ $p<0.05$ compared with the cuprizone group.

2.3.2.3 Cuprizone induces caspase-independent AIF-mediated cell death, which is attenuated by PARP-inhibition

Parallel to demyelination, we observed elevated expression of AIF in the CC of mice treated with cuprizone for 3 weeks, an effect that was attenuated by 4HQ (Fig. 6). Besides elevating its expression, cuprizone induced nuclear translocation of AIF. In cuprizone-treated mice, numerous cells showing typical shape and arrangement of OLs gave strong nuclear anti-AIF immunostaining in the midline and cingular part of the CC, which were prevented by the PARP inhibitor (Fig. 6). In contrast, cuprizone did not induce caspase-dependent cell death, as revealed by the absence of procaspase-3 cleavage determined by immunoblotting and a fluorescent caspase-3 assay (data not shown). Taken together, these data indicate caspase-independent AIF-mediated cell death in the CC of cuprizone-fed mice.

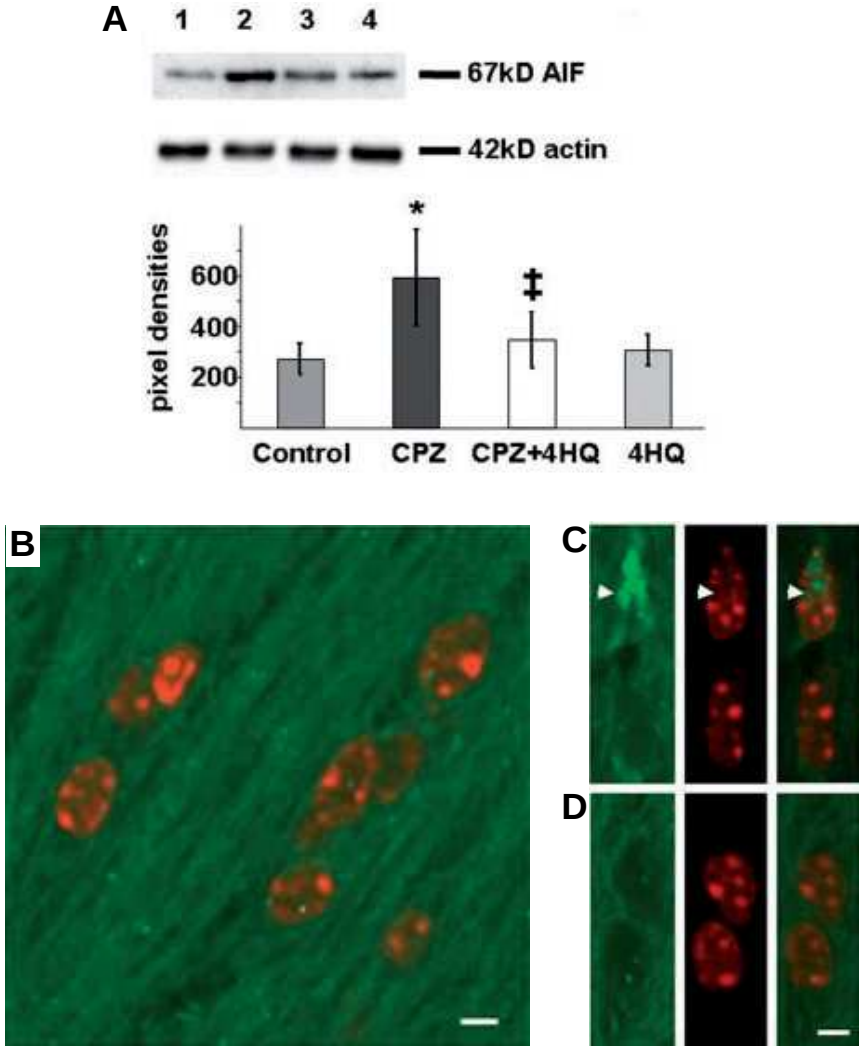

Figure 6. Effect of cuprizone and 4HQ treatment on the expression and nuclear translocation of AIF in the corpus callosum.
A: Expression of AIF in the dissected corpus callosum of mice treated for 3 weeks. Representative immunoblots and densitometric evaluations are shown. Lane 1 = control; lane 2 = cuprizone (CPZ) treatment; lane 3 = cuprizone and 4HQ (CPZ+4HQ) treatment; lane 4 =4HQ treatment. Results on the diagram are expressed as the mean pixel densities ± SD; *$p<0.05$ compared with control; ǂ$p<0.05$ compared with the cuprizone group.
B–D. Demonstration of nuclear translocation of AIF (green) by immunohistochemisty. Red represents nuclear counterstaining (DAPI). Confocal microscopy images were taken from representative areas of the midline of the corpus callosum of mice treated for 3 weeks. **B.** Representative merged image of untreated control mice (scale bar: 10 µm). **C and D.** Representative images of the green channel (left panels), the red channel (middle panel) and merged channels (right panel) of cuprizone (C) and cuprizone +4HQ (D) treated mice. Arrowheads indicate a cell where nuclear translocation of AIF occurred (scale bar: 10 µm).

2.3.2.4 Cuprizone activates Akt and mitogen-activated protein kinases in the corpus callosum and is modulated by inhibition of PARP

Three weeks of cuprizone feeding induced activation of the MAPKs, i.e. JNK, p38-MAPK and ERK1/2 and Akt indicated by immunoblotting utilizing phosphorylation-specific primary antibodies (Fig. 7). 4HQ treatment attenuated cuprizone-induced phosphorylation of JNK and p38-MAPK but not of ERK1/2 (Fig. 7). 4HQ alone did not affect phosphorylation of the MAPKs. In contrast to the effect on MAPKs, 4HQ enhanced cuprizone-induced phosphorylation of Akt. In addition, PARP inhibition alone also resulted in increased phosphorylation of Akt (Fig. 7).

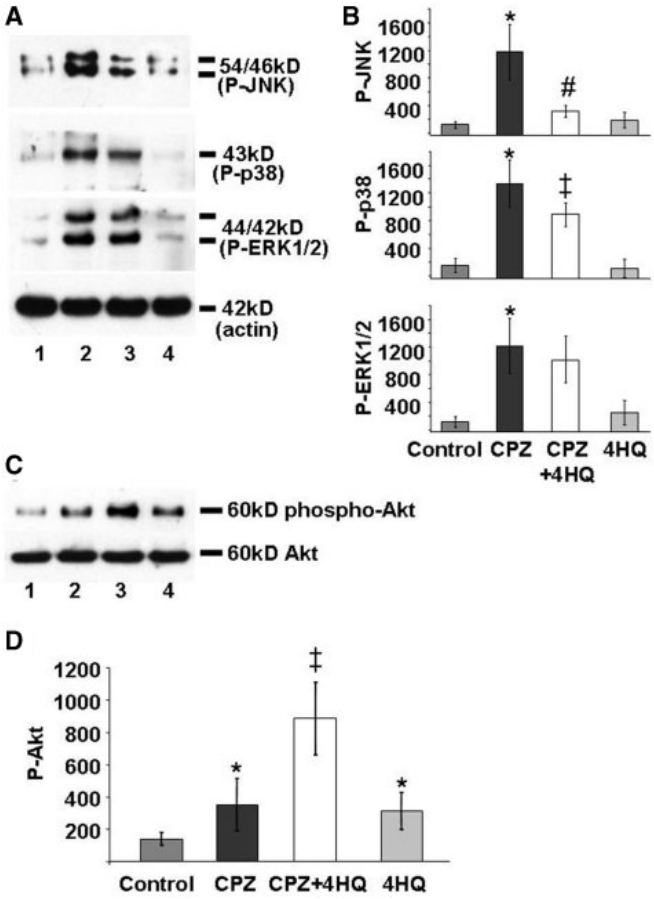

Figure 7. Effect of cuprizone and 4HQ treatment on the phosphorylation state of mitogen-activated protein kinases and Akt in the corpus callosum.
MAPK **(A and B)** and Akt **(C and D)** phosphorylation in the dissected corpus callosum of mice treated for 3 weeks was detected by immunoblotting utilizing phosphorylation-specific antibodies (P-Thr^{180}/Tyr^{182}- p38-MAPK, P-Thr^{183}/Tyr^{185} - JNK, P-Thr^{183}/Tyr^{185}- ERK1/2, P-Ser^{473} Akt).
Representative immunoblots (A and C) from three experiments (at least five mice in each group) and densitometric evaluations (B and D) are shown.
A and B Lane 1 = control; lane 2 = cuprizone (CPZ) treatment; lane 3 = cuprizone and 4HQ (CPZ+4HQ) treatment; lane 4 =4HQ treatment. Results on the diagram are expressed as mean pixel densities ±SD; *p<0.01 compared with control; #p<0.01 compared with the cuprizone group; ǂp<0.05 compared with cuprizone group.
C and D Lane 1 = control; lane 2 = cuprizone (CPZ) treatment; lane 3 = cuprizone and 4HQ (CPZ+4HQ) treatment; lane 4 =4HQ treatment. Results on the diagram are expressed as the mean pixel densities ±SD; *p<0.05 compared with control; ǂp<0.05 compared with the cuprizone group.

2.3.2.5 PARP activation in multiple sclerosis lesions

To determine PARP activation in MS lesions, we demonstrated accumulation of the enzyme's product by using anti-poly(ADP-ribose) immunofluorescence or immunohistochemistry. Poly(ADP-ribose)-positive cells were defined as cells with strong poly(ADP-ribose) immunoreactivity within the nuclei as well as in the cytoplasm, including cell processes; in the majority of these cells, poly(ADP-ribose)-positive nuclei appeared condensed and, in part, fragmented, suggesting apoptosis. In addition cytoplasmic poly(ADPribose) reactivity revealed signs of cell degeneration consistent with in part fragmented cell processes and cytoplasmic vacuolization. We observed very strong poly(ADP-ribose) reactivity in the nucleus and cytoplasm of single cells. This was most pronounced in patients with acute MS, in active lesions showing the characteristic pathological hallmarks of pattern III demyelination and containing high numbers of apoptotic OLs (Fig. 8 A–I). The expression was seen in cells that, by the anatomy of their processes, mainly resembled OLs (Fig. 8J–M and Fig. 9 A and B). They contained a condensed, sometimes fragmented nucleus and their cytoplasm revealed, in part, fragmented cell processes or swelling and focal vacuoles (Fig. 8L). In addition, a few cells with astrocyte or macrophage morphology also showed strong poly(ADP-ribose) immunoreactivity. On the other hand, both MS and control tissue demonstrated weak to-moderate labeling of nuclei for poly (ADP-ribose) (Fig. 8 J and M). This was highly variable between cases, and independent of lesions in MS tissue. The observation of variable and moderate PARP activation in post-mortem tissues may reflect agonal events. Quantitative analysis confirmed that poly(ADP-ribose) reactive glial cells were enriched in areas of initial and active myelin breakdown of pattern III lesions, as defined before [79](Table 3). Similar poly(ADP-ribose) reactive OLs, although in lower numbers, were also seen at the active edge of slowly expanding lesions in progressive MS (Fig. 8 S–V) and in lowest numbers in patients with pattern II lesions (Table 3). Double staining and confocal laser-scanning microscopy confirmed that the majority of cells with strong poly(ADP-ribose) immunoreactivity also expressed the OL marker carbonic anhydrase II (Fig. 9 C, E–H), but that

scattered cells also co-expressed poly(ADP-ribose) with either glial fibrillary acidic protein (Fig. 9 D) or CD68 (data not shown). Poly(ADP-ribose) reactivity in OLs exceeded that of astrocytes both in number of positive cells and intensity of the staining (Fig. 8 K, L, V and Fig. 9A, B).

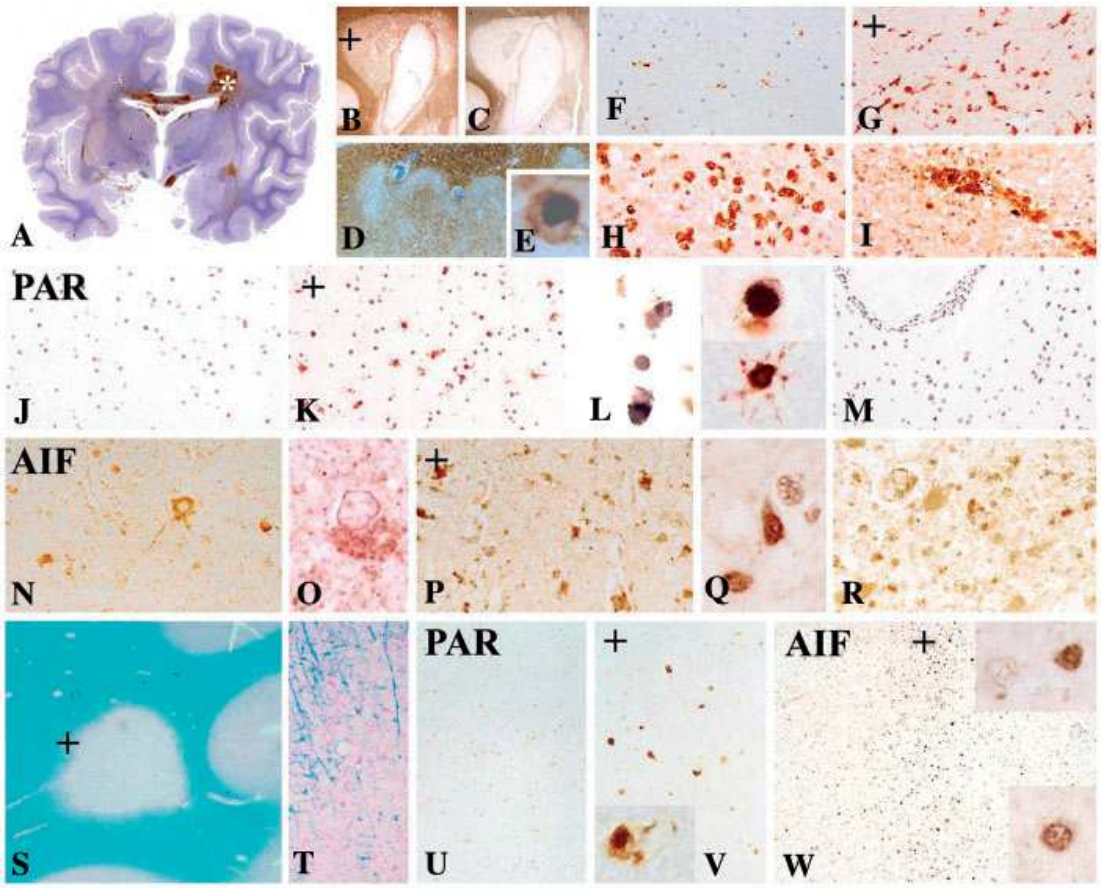

Figure 8. Activation of poly(ADP-ribose) polymerase (PAR) and nuclear translocation of AIF in different types of multiple sclerosis lesions **(A-M)**.

A–I Neuropathological characterization of multiple sclerosis pattern III lesions. A: Hemispheric brain section of patient P III C, stained by immunocytochemistry for macrophages/microglia (CD68), shows multiple active lesions within the brain; the asterisk labels the lesion shown in Figs B-L (x 0.3). Active pattern III lesion stained for myelin/oligodendrocyte glycoprotein (B) and MAG (C) showing loss of both myelin proteins in the centre of the lesion; in the very early lesion stages (+) MAG is completely lost from the lesion, while myelin/oligodendrocyte glycoprotein expression is partly preserved (x1.2). D: Very early stage of pattern III lesion shows partial loss of myelin (stained for proteolipid protein), however, the inflamed vessels are surrounded by rim of preserved myelin (x 40). E: Within the active lesion oligodendrocytes that are stained for cyclic nucleotide phosphodiesterase show condensed nuclei reminiscent of apoptosis (x 1200).

F: Staining for CD68 shows only few activated microglia cells in the normal appearing white matter. G: a profound increase of activated microglia in early lesions showing selective loss of MAG. H: profound infiltration of the tissue with macrophages in late active portions of the lesion, and I: mainly perivascular accumulation of macrophages in the inactive lesion centre (x 200).

Poly(ADP-ribose) expression in different lesion stages from the case shown in (A–I); J: in the normal appearing white matter there is faint brown nuclear staining of glial cells; the nuclei are counterstained with haematoxylin (blue). K: in the area of MAG loss (the '+' indicates the location of the area in B), numerous cells are seen with intense nuclear and cytoplasmic reactivity for poly(ADP-ribose); L: higher magnification of the cells shows different examples of poly(ADP-ribose) positive glial cells with dark condensed nuclei and partial cytoplasmic or cell process dissolution; M: the lesion centre shows weak brown immunoreactivity in some nuclei, similar to that seen in the normal-appearing white matter (x 200; inserts x 1200). (Continued on next page.)

Figure 8. Activation of poly(ADP-ribose) polymerase (PAR) and nuclear translocation of AIF in different types of multiple sclerosis lesions. **(N-W)**
AIF expression in similar lesion areas of the same case shown for poly(ADP-ribose) before; N, O: purely mitochondrial AIF expression in the normal appearing white matter; P, Q: in the early active (MAG loss) lesions AIF is seen not only in mitochondria, but also in nuclei; R: in the inactive lesion centre AIF is only present in mitochondria (x 200; inserts x 1200).
Poly(ADP-ribose) and AIF expression in a slowly expanding lesion in progressive multiple sclerosis (ChMS D); S shows the location of the lesion in the subcortical white matter (x 4) and T documents the hypercellular margin of the lesions with some macrophages with recent myelin degradation products (x 100); no poly(ADP-ribose) expression was seen in the normal appearing white matter (U); however, there is a moderate number of small oligodendrocyte like glia cells with strong poly(ADP-ribose) reactivity within condensed nuclei and cell processes in V; the + labels the active lesion area in S, V and W. W: AIF expression is enriched in the area of active lesion expansion (+); in the majority of the cells AIF is seen as cytoplasmic granules, representing mitochondria (upper insert), but there is also AIF reactivity in nuclei of cells, resembling oligodendrocytes (lower insert) (x 200).

2.3.2.6 Nuclear translocation of AIF in pattern III multiple sclerosis lesions

Since AIF is essential in mediating PARP-dependent cell death [69], we examined its expression in MS lesions. AIF reactivity in the normal brain, and with some exceptions in the normal appearing white matter of MS patients (Table 3) was confined to the mitochondria of neurons and glia cells (Fig. 8 N, O). In MS lesions, AIF reactivity in mitochondria was enhanced (Fig. 8 P–R, W) and seen not only in neurons and glia but also in macrophages. Within initial and active areas of MS pattern III lesions and much less in other active MS lesions (Table 3), we found a variable number of glia cells with nuclear AIF reactivity (Fig. 8 P, Q and W) co-localized with increased anti-poly(ADP-ribose) staining in condensed nuclei, showing features of apoptosis (Fig. 9I–L). These data suggested that activation of PARP may result in AIF-mediated OL death in pattern III MS lesions.

Table 3. Poly(ADP-ribose) and nuclear AIF expression in multiple sclerosis

Table 3				
Samples	MS III	MS II	Progressive	Controls
Cases	4	3	6	7
PAR early	71.4±27.0***	1.6±1.7	15.3±9.2**	n.a.
PAR IA	22.2±17.9**	0.2±0.4	4.6±7.3	n.a.
PAR NWM	5.0±7.4	0.8±0.7	1.4±1.4	0.6±0.7
AIF early	19.1±7.7***	2.5±2.8*	11.9±5.0***	n.a.
AIF IA	9.0±5.4**	2.5±2.3	3.3±3.8	n.a.
AIF NWM	4.9±2.5***	1.0±1.7	2.2±2.6	0.2±0.1

Quantitative analysis of cells with poly(ADP-ribose) immunoreactivity and nuclear AIF expression in glial cells in different types of multiple sclerosis lesions.
The cases are identical to those described in Table 1; MS III = multiple sclerosis patients with pattern III lesions; MS II = multiple sclerosis cases with pattern II lesions; progressive = multiple sclerosis cases with slowly expanding lesions of progressive multiple sclerosis; PAR = poly(ADP-ribose); NWM= normal white matter.
The numbers represent cells with positive immunoreactivity/mm^2. Mean ± SD in normal white matter, in early lesions of multiple sclerosis pattern III cases or at sites of initial myelin destruction in pattern II lesions or slowly expanding lesions in progressive multiple sclerosis (early), and in the centre of the lesions that still contained macrophages with myelin degradation products at different stages of digestion (IA). Significant difference from respective control normal white matter values was indicated *p<0.05, **p<0.01 and ***p<0.001.

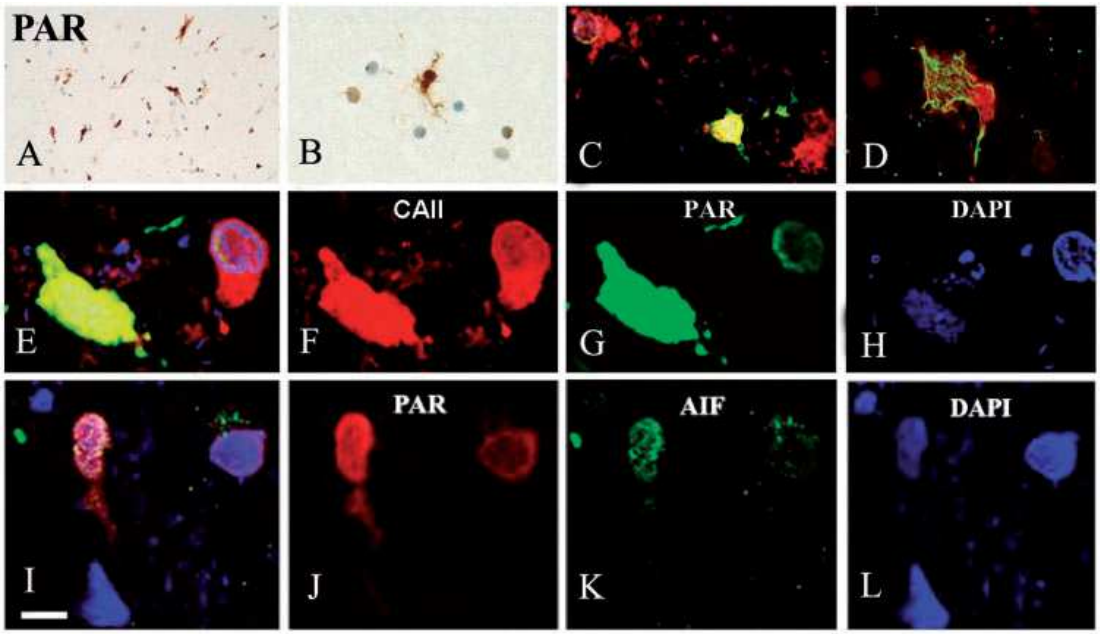

Figure 9. Activation of poly(ADP-ribose) polymerase and nuclear translocation of AIF in active pattern III multiple sclerosis lesions.

A–H: Examples of poly(ADP-ribose) (PAR) reactivity within glial cells of active pattern III lesions (within the area of MAG loss), demonstrated by confocal microscopy double labeling for poly(ADP-ribose) (PAR) and carbonic anhydrase II (CAII) within an oligodendrocyte (C), for poly(ADP-ribose) and glial fibrillary acidic protein in an astrocyte (D) and triple labelling for carbonic anhydrase II (CAII; red; F), poly(ADPribose) (green; G) and DAPI (blue nuclei, H) in oligodendrocytes at different stages of degeneration; (E) shows the overlay of triple staining (x 1200).

I–L: Representative confocal images of nuclear co-localization of poly(ADP-ribose) and AIF. poly(ADP-ribose) immunoreactivity (red), AIF immunoreactivity (green) and DAPI nuclear staining (blue) were presented individually and merged (I) (scale bar: 10 µm).

2.4 Discussion

In our first study we aimed to investigate the role of gonadal steroids during experimentally-induced demyelination in the male CC using cuprizone as toxic agent. We provide here clear evidence that the application of both ovarian steroids, E and P, possess the capacity of inhibiting mature OL damage and/or of positively stimulating (re)myelination, whereas single steroid treatments did not exceed mild effects. Moreover, both hormones appeared to balance the interaction of astroglia, microglia, and/or OL and OL precursors resulting in a strong activation of resting premature OLs or prevention of mature oligodendrocyte damage. The activation and differentiation of premature OLs is assumed to be the major account for the observed counteraction of cuprizone induced demyelination by sex steroids.

The influence of pregnancy and hormonal substitution on the course of demyelination and disease progress in MS and in experimental models for MS is well-documented [51]. It appears, at first glance, from experimental studies that E or estrogen-derivates such as estriol are the protective factors [53-55]. The role of P in MS has been controversial. In one study, P-attenuated disease severity in experimental allergic encephalomyelitis (EAE) [56], another study, however, reported a worse outcome induced by P administration in the same animal model [57]. Although experimental evidence is supportive for a protective role of steroids during MS, the related cellular events in affected brain areas remain unknown or are only partially understood. Both hormones are known to affect and regulate a large number of cell protective mechanisms [48, 49, 82-84]. A number of immunological parameters are altered during pregnancy, for example, the shift from a primary pro-inflammatory Th1 response to an anti-inflammatory Th2 response [85]. Therefore, it was postulated that the beneficial effects of E and P in MS patients may result from direct modulation of the adaptive immune system. However, in cuprizone induced demyelination, an invasion of T- or B cells is not observed [86]. Therefore, our study clearly shows that E and P treatment is also

protective during demyelination independent of a B- and T cell- initiated autoimmune reaction. This might be of particular interest during progressive MS courses where involvement of B- and T-cells is rarely detectable [87]. Thus, an interaction with other immune cells such as macrophages, resident microglia, and astrocytes might be responsible for protective hormonal effects.

The accumulation of macrophages is a well-known feature in cuprizone induced demyelination [36, 86, 88]). The specific role of macrophages in MS is still controversial and there is good evidence that macrophages have both neuroprotective and neurodegenerative functions. In vitro studies reported an increased neuronal damage through activated microglia [53]. Other reports support the concept that pro-inflammatory cytokines produced by microglia are neuroprotective as shown by the up-regulation of excitotoxicity in tumor necrosis factor-α and interleukin-1β knockout mice [89]. Macrophages may also support remyelination. Depletion of macrophages impairs remyelination after lysolecithin-induced demyelination [90]. In particular, macrophages are beneficial during early phases of remyelination. In cuprizone-mediated demyelination, the recruitment of macrophages is most obvious in areas with distinct demyelination like the lateral part of the CC [43, 86]. The medial part is usually less demyelinated and, in consequence, macrophage invasion is less manifested. In E/P-treated animals, we observed a massive infiltration of macrophages in the lateral part but also in the midline of the CC. Although the contribution of activated macrophages to demyelination and remyelination is not yet solved, the ‘‘shift’’ of macrophage localization may have a decisive impact in the mediation of protective hormonal effects. Activated microglia can phagocytose debris and produce cytokines/growth factors that stimulate OL precursor cells [43]. Therefore, the mobilization of macrophages in the midline of the CC may be of particular interest. In general, protective hormonal effects might be the consequence of a reduced demyelination or an increased remyelination during the 5 weeks of cuprizone administration. Our data support the latter view. We demonstrate that both hormones are required to induce the expression of myelin forming proteins such as MBP and PLP which are massively reduced after cup-treatment. In our study, we have used steroid doses

yielding moderate steroid plasma levels resembling those of pregnant mice at the beginning of the last trimester. This shows that sub-toxic steroid levels can achieve protective effects. However, we have not applied higher steroid doses which may have a higher therapeutic effect. Myelin proteins such as MBP are primarily responsible for adhesion of the cytosolic surfaces to multilayered compact myelin sheets [91, 92]. It is the only structural protein found so far to be essential for the formation of CNS myelin, and is regarded as the ‘‘executive’’ molecule of myelin [91]. Which mechanisms are responsible for the formation of new myelin? We show that the hormonal treatment accounts for higher levels of PDGFα-R, a marker for OL precursors, and higher numbers of Ki-67-immunopositive proliferating cells in all parts of the CC. The recruitment of new OLs could be the result of stimulated astrogliosis and, subsequently, IGF-1 synthesis and release by astrocytes as observed in our study. IGF-1 is important for OL differentiation, maturation, and myelin formation but also can interact with mature OLs thereby preventing cell death under different toxic conditions [93-96]. It is well established that IGF-1 and sex steroids are interconnected in the brain. Cross-talk between those compounds has been described in reproductive tissues and the CNS [97, 98]. Most importantly, such mutual reactions have been shown to play a critical role in the inhibition of damaging processes and neuroprotection in the brain [99]. IGF-1 and steroid interactions in the brain appear to be reciprocally. Receptors for estrogen and IGF-1 are cross-regulated in neural tissue, and astroglia often coexpresses both. In addition, E can activate IGF-1 receptors most likely via estrogen receptor-alpha [100]. This type of estrogen receptor is present in astrocytes [101] and preliminary observations in our cuprizone animal model reveal a high presence of this receptor subtype in the injured CC. Although the importance of IGF-1 for the recovery from injuries in the brain is widely accepted, we may speculate that other not yet identified factors are involved in this scenario.

In conclusion our data implicate that E and P abolish destructive cuprizone effects in the brain by stimulating OL activation and/or remyelination. Therefore, a therapeutic application of both hormones rather than single hormone usage comes

into question for MS. Because the cuprizone model for demyelination represents more aspects of the chronic progressive MS forms, the clinical use of the hormones should be selectively considered. In this regard, it needs to be emphasized that remyelination protects axons from demyelination associated axonal degeneration [86, 102].
The understanding of the impact of hormone-administration on remyelination, axonal protection, neurodegeneration, and, in consequence, clinical outcome in this animal model is of particular clinical relevance and has to be addressed in further experiments.

In our second set of experiments, we used cuprizone induced demyelination as an animal model for OL depletion, as observed in MS, and its prevention by PARP inhibition. Demyelination and OL death are general features of MS, which have even been suggested to be the primary events in lesion evolution, and may contribute to chronic inflammation through epitope spreading and axonal degeneration, which correlates with clinical disability [103]. On the other hand, OL injury and tissue destruction may be the consequence of the inflammatory process of MS [104, 105] Regardless of the primary trigger for OL death in MS, mitochondrial dysfunction with subsequent apoptotic cell death is a cardinal feature in at least a subset of acute and chronic MS lesions [64, 65] and this feature is shared between the cuprizone model and MS. Mitochondrial dysfunction with excessive reactive oxygen species production suggested by previous studies [37, 44, 66, 67, 106] could cause the PARP activation observed by us of degenerating OLs in the cuprizone model and active pattern III MS lesions. Overactivation of PARP promotes cell death by ATP depletion in the cell and regulating the release of AIF from mitochondria [68, 69]. AIF then translocates to the nucleus, leading to chromatin condensation, large-scale DNA fragmentation (450 kb) and cell death in a caspase-independent manner [107, 108]. In fact, we observed nuclear translocation of AIF co-localized with poly(ADP-ribose) in several OLs in both pattern III MS lesions and the cuprizone model. However, we were unable to detect caspase-3 activation in the corpus callosum of cuprizone-treated mice in agreement with previous findings [44, 109]. Specificity and possible

side-effects of a pharmacological agent are always an issue. However, 4HQ was reported to have a high potency for PARP-1 and no effects on enzymes other than PARP have been documented [77]. Therefore, it seems likely that diminished demyelination and OL loss induced by cuprizone can be assigned to the PARP inhibitory effect of 4HQ. JNK and p38-MAPK activation are considered to promote cell death [107, 110-112]. Indeed, we observed that cuprizone increased phosphorylation of JNK and p38-MAPK in the CC, which was attenuated upon PARP inhibition. Cuprizone also induced ERK1/2 activation in the corpus callosum but it was not affected by the PARP inhibitor 4HQ, which can be explained by the notion that the MAPK/ERK kinase-ERK1/2 pathway is upstream to PARP activation [113, 114]. Since ERK activation was found to promote OL survival [115, 116], cuprizone-induced ERK activation may represent a protective mechanism against OL death. In conclusion, all effects of PARP inhibition on the MAPK pathways, i.e. suppressing JNK and p38 activation while not affecting ERK, could promote OL survival. Cuprizone intoxication also resulted in Akt phosphorylation, which was further enhanced by co-administration of 4HQ. Furthermore, PARP inhibition alone caused phosphorylation of Akt in accordance with previous findings [70, 117]. Activation of Akt prevented neuronal apoptosis by inhibiting translocation of AIF to the nucleus [53], protected oligodendrocytes against tumor necrosis factor-induced apoptosis [118] and, by phosphorylating their respective upstream kinases, decreased activity of JNK and p38-MAPK [119, 120]. Based on these data, our results may suggest that in response to cuprizone, the cytoprotective phosphatidylinositol-3 kinase/Akt pathway became activated, although it was insufficient to prevent OL death. Additional activation by PARP inhibition could be sufficient to protect OLs against apoptosis, mediated partially by reduced activation of JNK and p38-MAPK and maintaining the integrity of the mitochondrial membrane systems preventing nuclear translocation of AIF. Besides the pathological similarities (primary OL apoptosis associated with microglia activation, minor or absent humoral or cellular immune response) we observed identical patterns of at least two key molecular mechanisms, i.e. PARP activation and caspase-independent AIF-mediated apoptosis of OLs in both pattern III

multiple sclerosis lesions and cuprizone induced demyelination. These data may suggest that the apoptosis of OLs, at least in a subgroup of MS patients and in the cuprizone model, happens via similar pathways. Thus, inhibition of PARP may be similarly effective in MS and may have several important aspects. By blocking demyelination, PARP inhibition may reduce inflammation through preventing epitope spreading. In addition, as indicated by EAE experiments [76], it also has a direct, beneficial effect on inflammation. Inhibiting PARP may thus influence degenerative and autoimmune inflammatory processes in MS and provide an effective therapy targeting two basic mechanisms at the same time. Recently, plasma exchange has been shown to be highly efficient in patients with antibody-mediated pattern II lesions indicating the importance of mechanism-specific treatment strategies [121]. Similarly, PARP-inhibitors may be effective in patients with pattern III lesions characterized by primary OL death. In summary, our data indicate that OL death occurs via very similar mitochondrial pathomechanisms in the cuprizone model and pattern III MS lesions. Inhibition of PARP effectively attenuated OL depletion and protected against experimental demyelination mediated through a caspase-independent pathway involving nuclear translocation of AIF. Considering that PARP inhibition was also highly effective in EAE, the autoimmune inflammatory model of MS, it may provide a therapeutic approach protecting against two basic processes in MS, inflammation and demyelination. Moreover, it may target all subtypes of MS either by preventing OL death, a key event in the formation of all new lesions or additionally, by targeting inflammation.

Although the immune-modulator treatments are proved to reduce the frequency of relapses in MS, it is only effective in about 50-60% of patients with the relapsing-remitting form of the disease (40-50% of the patients are “non responders”). In certain amount of patients (primary progressive, secondary progressive) currently available treatments are proved to be ineffective. The immune-modulator treatments target only the immune mediated processes of MS, although it has been established that type III and type IV MS subtypes are characterized mostly by OL apoptosis and loss resembling of rather a neurodegenerative disease.

Therefore there is a paramount need to discover new approaches of treatment for the non-immune mediated aspects of MS.

In our experiments we showed evidences that sexual steroid treatment and the inhibition of OL apoptosis by PARP inhibitor are efficient to prevent demyelination in a model of non-immune mediated MS characterized by OL apoptosis and primary demyelination. Additionally, our data suggest that these different therapeutical approaches target different pathomechanisms of OL apoptosis; the combined gonadal steroid treatment promotes OL maturation i.e. remyelination, while PARP inhibition promotes OL survival and prevents the apoptosis of these cells. Based on these findings we assume that targeting different mechanisms of OL apoptosis by a combined sexual steroid/PARP inhibitor treatment might provide an effective therapy for those patients who do not respond to the currently available medications for MS.

3 Summary of the thesis

MS is the most common neurological disease of the young adulthood in the Western hemisphere. Although immune-modulator treatments have achieved some progress in the treatment of percentage of MS patients, these therapies have no useful treatment effect e.g. on the secondary progressive phase of the disease [122-124]. Likewise, no agent has been shown to affect primary progressive MS [125].

In addition, it has been revealed that the pathophysiology of MS is heterogeneous [6], and it has been suggested, that different pathological subtypes of MS may require different therapeutical approaches.

In this study - by using a mouse model that mimics pattern III MS subtype - we aimed to explore new therapeutical approaches to MS forms mainly characterized by OL apoptosis either by promoting the remyelination process or by inhibiting the apoptosis of mature OLs. Additionally, our goal was to investigate pathomechanisms that may have a role in OL loss in MS.

3.1 Effect of 17β-estradiol and progesterone treatment on cuprizone induced demyelination in C57BL/6 mice

- In vivo MRI investigation, routine histopathology and immunohystochemistry revealed that mice administered the combined hormone therapy have a better myelin status than the cuprizone treated mice.

- Combined hormone therapy induced massive astrocyte reaction and macrophage accumulation during the cuprizone challenge. Astrocytosis and macrophage activation are well known features of the cuprizone induced demyelination, but the hormone treatment strongly enhanced these reactions.

- The administration of 17β-estradiol and progesterone induced the expression of remyelination-related genes (IGF-1 and PDGF-alpha R) in the corpus callosum of cuprizone treated mice. Additionally, hormone treated mice revealed more dividing cells in the subventricular zone.

- Our data implicate that the combined hormone therapy promote the maturation of OL precursors and thus the remyelination in the cuprizone induced demyelination model.

- Our results suggest that a combined17β-estradiol and progesterone hormone therapy might have a beneficial role in the non-immune mediated forms of MS.

3.2 Effect of poly(ADP-ribose) polymerase inhibition on cuprizone induced demyelination

- Cuprizone administration induces PARP activation, and this effect is attenuated by the administration of the PARP inhibitor 4HQ.
- Through PARP overactivation, cuprizone induces AIF mediated, caspase-independent apoptosis of OLs.
- Inhibition of the nuclear enzyme PARP by 4HQ treatment diminishes the demyelination induced by cuprizone, as demonstrated by in vivo MRI, histology, immunohystochemistry and immunoblot analysis.
- PARP inhibition provides a protective effect on OL apoptosis and thus attenuates demyelination in the cuprizone model.
- PAR overactivation and consequent AIF mediated, caspase independent OL apoptosis is present in type III MS lesions.
- Our data indicate that PARP inhibition might provide a therapeutic approach against OL death in MS.

4 References

1. Rosati, G., *The prevalence of multiple sclerosis in the world: an update.* Neurol Sci, 2001. **22**(2): p. 117-39.
2. Compston, A. and A. Coles, *Multiple sclerosis.* Lancet, 2008. **372**(9648): p. 1502-17.
3. Alonso, A. and M.A. Hernan, *Temporal trends in the incidence of multiple sclerosis: a systematic review.* Neurology, 2008. **71**(2): p. 129-35.
4. Noseworthy, J.H., et al., *Multiple sclerosis.* N Engl J Med, 2000. **343**(13): p. 938-52.
5. Vecsei, L. and S. Komoly, *Sclerosis Multiplex*2003, Hungary: Therapia Kiado.
6. Lucchinetti, C., et al., *Heterogeneity of multiple sclerosis lesions: implications for the pathogenesis of demyelination.* Ann Neurol, 2000. **47**(6): p. 707-17.
7. Consortium, I.M.S.G., *Refining genetic associations in multiple sclerosis.* Lancet Neurol, 2008. **7**(7): p. 567-9.
8. Marrie, R.A., *Environmental risk factors in multiple sclerosis aetiology.* Lancet Neurol, 2004. **3**(12): p. 709-18.
9. Lucchinetti, C.F., et al., *Distinct patterns of multiple sclerosis pathology indicates heterogeneity on pathogenesis.* Brain Pathol, 1996. **6**(3): p. 259-74.
10. Barnett, M.H. and J.W. Prineas, *Relapsing and remitting multiple sclerosis: pathology of the newly forming lesion.* Ann Neurol, 2004. **55**(4): p. 458-68.
11. Henderson, A.P., et al., *Multiple sclerosis: distribution of inflammatory cells in newly forming lesions.* Ann Neurol, 2009. **66**(6): p. 739-53.
12. Barnett, M.H. and I. Sutton, *The pathology of multiple sclerosis: a paradigm shift.* Curr Opin Neurol, 2006. **19**(3): p. 242-7.
13. Breij, E.C., et al., *Homogeneity of active demyelinating lesions in established multiple sclerosis.* Ann Neurol, 2008. **63**(1): p. 16-25.
14. Trapp, B.D., et al., *Axonal transection in the lesions of multiple sclerosis.* N Engl J Med, 1998. **338**(5): p. 278-85.
15. Lovas, G., et al., *Axonal changes in chronic demyelinated cervical spinal cord plaques.* Brain, 2000. **123 (Pt 2)**: p. 308-17.
16. Anderson, J.M., et al., *Abnormally phosphorylated tau is associated with neuronal and axonal loss in experimental autoimmune encephalomyelitis and multiple sclerosis.* Brain, 2008. **131**(Pt 7): p. 1736-48.
17. Kutzelnigg, A., et al., *Cortical demyelination and diffuse white matter injury in multiple sclerosis.* Brain, 2005. **128**(Pt 11): p. 2705-12.
18. Magliozzi, R., et al., *Meningeal B-cell follicles in secondary progressive multiple sclerosis associate with early onset of disease and severe cortical pathology.* Brain, 2007. **130**(Pt 4): p. 1089-104.
19. Stadelmann, C., *Multiple sclerosis as a neurodegenerative disease: pathology, mechanisms and therapeutic implications.* Curr Opin Neurol, 2011. **24**(3): p. 224-9.
20. Patrikios, P., et al., *Remyelination is extensive in a subset of multiple sclerosis patients.* Brain, 2006. **129**(Pt 12): p. 3165-72.

21. Scolding, N., et al., *Oligodendrocyte progenitors are present in the normal adult human CNS and in the lesions of multiple sclerosis.* Brain, 1998. **121 (Pt 12)**: p. 2221-8.
22. Geurts, J.J. and F. Barkhof, *Grey matter pathology in multiple sclerosis.* Lancet Neurol, 2008. **7**(9): p. 841-51.
23. Allen, I.V., et al., *Pathological abnormalities in the normal-appearing white matter in multiple sclerosis.* Neurol Sci, 2001. **22**(2): p. 141-4.
24. Kornek, B. and H. Lassmann, *Axonal pathology in multiple sclerosis. A historical note.* Brain Pathol, 1999. **9**(4): p. 651-6.
25. Friese, M.A., et al., *The value of animal models for drug development in multiple sclerosis.* Brain, 2006. **129**(Pt 8): p. 1940-52.
26. Lassmann, H., *Experimental models of multiple sclerosis.* Rev Neurol (Paris), 2007. **163**(6-7): p. 651-5.
27. Mix, E., H. Meyer-Rienecker, and U.K. Zettl, *Animal models of multiple sclerosis for the development and validation of novel therapies - potential and limitations.* J Neurol, 2008. **255 Suppl 6**: p. 7-14.
28. Wekerle, H., *Lessons from multiple sclerosis: models, concepts, observations.* Ann Rheum Dis, 2008. **67 Suppl 3**: p. iii56-60.
29. Oleszak, E.L., et al., *Theiler's virus infection: a model for multiple sclerosis.* Clin Microbiol Rev, 2004. **17**(1): p. 174-207.
30. Blakemore, W.F. and R.J. Franklin, *Remyelination in experimental models of toxin-induced demyelination.* Curr Top Microbiol Immunol, 2008. **318**: p. 193-212.
31. Carlton, W.W., *Response of mice to the chelating agents sodium diethyldithiocarbamate, alpha-benzoinoxime, and biscyclohexanone oxaldihydrazone.* Toxicol Appl Pharmacol, 1966. **8**(3): p. 512-21.
32. Carlton, W.W., *Studies on the induction of hydrocephalus and spongy degeneration by cuprizone feeding and attempts to antidote the toxicity.* Life Sci, 1967. **6**(1): p. 11-9.
33. Blakemore, W.F., *Observations on oligodendrocyte degeneration, the resolution of status spongiosus and remyelination in cuprizone intoxication in mice.* J Neurocytol, 1972. **1**(4): p. 413-26.
34. Blakemore, W.F., *Demyelination of the superior cerebellar peduncle in the mouse induced by cuprizone.* J Neurol Sci, 1973. **20**(1): p. 63-72.
35. Komoly, S., et al., *Decrease in oligodendrocyte carbonic anhydrase activity preceding myelin degeneration in cuprizone induced demyelination.* J Neurol Sci, 1987. **79**(1-2): p. 141-8.
36. Komoly, S., et al., *Insulin-like growth factor I gene expression is induced in astrocytes during experimental demyelination.* Proc Natl Acad Sci U S A, 1992. **89**(5): p. 1894-8.
37. Ludwin, S.K., *Central nervous system demyelination and remyelination in the mouse: an ultrastructural study of cuprizone toxicity.* Lab Invest, 1978. **39**(6): p. 597-612.
38. Matsushima, G.K. and P. Morell, *The neurotoxicant, cuprizone, as a model to study demyelination and remyelination in the central nervous system.* Brain Pathol, 2001. **11**(1): p. 107-16.

39. Lindner, M., et al., *Chronic toxic demyelination in the central nervous system leads to axonal damage despite remyelination.* Neurosci Lett, 2009. **453**(2): p. 120-5.
40. Kalman, B., K. Laitinen, and S. Komoly, *The involvement of mitochondria in the pathogenesis of multiple sclerosis.* J Neuroimmunol, 2007. **188**(1-2): p. 1-12.
41. Komoly, S., *Experimental demyelination caused by primary oligodendrocyte dystrophy. Regional distribution of the lesions in the nervous system of mice [corrected].* Ideggyogy Sz, 2005. **58**(1-2): p. 40-3.
42. Kipp, M., et al., *The cuprizone animal model: new insights into an old story.* Acta Neuropathol, 2009. **118**(6): p. 723-36.
43. Remington, L.T., et al., *Microglial recruitment, activation, and proliferation in response to primary demyelination.* Am J Pathol, 2007. **170**(5): p. 1713-24.
44. Pasquini, L.A., et al., *The neurotoxic effect of cuprizone on oligodendrocytes depends on the presence of pro-inflammatory cytokines secreted by microglia.* Neurochem Res, 2007. **32**(2): p. 279-92.
45. Lindner, M., et al., *Sequential myelin protein expression during remyelination reveals fast and efficient repair after central nervous system demyelination.* Neuropathol Appl Neurobiol, 2008. **34**(1): p. 105-14.
46. Armstrong, R.C., *Growth factor regulation of remyelination: behind the growing interest in endogenous cell repair of the CNS.* Future Neurol, 2007. **2**(6): p. 689-697.
47. Morell, P., et al., *Gene expression in brain during cuprizone-induced demyelination and remyelination.* Mol Cell Neurosci, 1998. **12**(4-5): p. 220-7.
48. Garcia-Segura, L.M., I. Azcoitia, and L.L. DonCarlos, *Neuroprotection by estradiol.* Prog Neurobiol, 2001. **63**(1): p. 29-60.
49. Kipp, M., et al., *Estrogen and the development and protection of nigrostriatal dopaminergic neurons: concerted action of a multitude of signals, protective molecules, and growth factors.* Front Neuroendocrinol, 2006. **27**(4): p. 376-90.
50. Dwosh, E., et al., *The interaction of MS and pregnancy: a critical review.* Int MS J, 2003. **10**(2): p. 38-42.
51. Voskuhl, R.R., *Hormone-based therapies in MS.* Int MS J, 2003. **10**(2): p. 60-6.
52. Worthington, J., et al., *Pregnancy and multiple sclerosis--a 3-year prospective study.* J Neurol, 1994. **241**(4): p. 228-33.
53. Kim, S., et al., *Estriol ameliorates autoimmune demyelinating disease: implications for multiple sclerosis.* Neurology, 1999. **52**(6): p. 1230-8.
54. Sicotte, N.L., et al., *Treatment of multiple sclerosis with the pregnancy hormone estriol.* Ann Neurol, 2002. **52**(4): p. 421-8.
55. Soldan, S.S., et al., *Immune modulation in multiple sclerosis patients treated with the pregnancy hormone estriol.* J Immunol, 2003. **171**(11): p. 6267-74.
56. Garay, L., et al., *Effects of progesterone in the spinal cord of a mouse model of multiple sclerosis.* J Steroid Biochem Mol Biol, 2007. **107**(3-5): p. 228-37.
57. Hoffman, G.E., et al., *Divergent effects of ovarian steroids on neuronal survival during experimental allergic encephalitis in Lewis rats.* Exp Neurol, 2001. **171**(2): p. 272-84.
58. Gibson, C.L., et al., *Progesterone for the treatment of experimental brain injury; a systematic review.* Brain, 2008. **131**(Pt 2): p. 318-28.

59. Offner, H. and M. Polanczyk, *A potential role for estrogen in experimental autoimmune encephalomyelitis and multiple sclerosis.* Ann N Y Acad Sci, 2006. **1089**: p. 343-72.
60. Palaszynski, K.M., et al., *Estriol treatment ameliorates disease in males with experimental autoimmune encephalomyelitis: implications for multiple sclerosis.* J Neuroimmunol, 2004. **149**(1-2): p. 84-9.
61. Bruck, W., C. Lucchinetti, and H. Lassmann, *The pathology of primary progressive multiple sclerosis.* Mult Scler, 2002. **8**(2): p. 93-7.
62. Kleinschnitz, C., et al., *Multiple sclerosis therapy: an update on recently finished trials.* J Neurol, 2007. **254**(11): p. 1473-90.
63. Frohman, E.M., M.K. Racke, and C.S. Raine, *Multiple sclerosis--the plaque and its pathogenesis.* N Engl J Med, 2006. **354**(9): p. 942-55.
64. Aboul-Enein, F., et al., *Preferential loss of myelin-associated glycoprotein reflects hypoxia-like white matter damage in stroke and inflammatory brain diseases.* J Neuropathol Exp Neurol, 2003. **62**(1): p. 25-33.
65. Mahad, D., et al., *Mitochondrial defects in acute multiple sclerosis lesions.* Brain, 2008. **131**(Pt 7): p. 1722-35.
66. Suzuki, K., *Giant hepatic mitochondria: production in mice fed with cuprizone.* Science, 1969. **163**(862): p. 81-2.
67. Turrens, J.F., *Mitochondrial formation of reactive oxygen species.* J Physiol, 2003. **552**(Pt 2): p. 335-44.
68. Alano, C.C., W. Ying, and R.A. Swanson, *Poly(ADP-ribose) polymerase-1-mediated cell death in astrocytes requires NAD+ depletion and mitochondrial permeability transition.* J Biol Chem, 2004. **279**(18): p. 18895-902.
69. Yu, S.W., et al., *Mediation of poly(ADP-ribose) polymerase-1-dependent cell death by apoptosis-inducing factor.* Science, 2002. **297**(5579): p. 259-63.
70. Tapodi, A., et al., *Pivotal role of Akt activation in mitochondrial protection and cell survival by poly(ADP-ribose)polymerase-1 inhibition in oxidative stress.* J Biol Chem, 2005. **280**(42): p. 35767-75.
71. Xu, Y., et al., *Poly(ADP-ribose) polymerase-1 signaling to mitochondria in necrotic cell death requires RIP1/TRAF2-mediated JNK1 activation.* J Biol Chem, 2006. **281**(13): p. 8788-95.
72. Oliver, F.J., et al., *Resistance to endotoxic shock as a consequence of defective NF-kappaB activation in poly (ADP-ribose) polymerase-1 deficient mice.* EMBO J, 1999. **18**(16): p. 4446-54.
73. Kauppinen, T.M. and R.A. Swanson, *The role of poly(ADP-ribose) polymerase-1 in CNS disease.* Neuroscience, 2007. **145**(4): p. 1267-72.
74. Endres, M., et al., *Ischemic brain injury is mediated by the activation of poly(ADP-ribose)polymerase.* J Cereb Blood Flow Metab, 1997. **17**(11): p. 1143-51.
75. Mandir, A.S., et al., *NMDA but not non-NMDA excitotoxicity is mediated by Poly(ADP-ribose) polymerase.* J Neurosci, 2000. **20**(21): p. 8005-11.
76. Scott, G.S., et al., *The therapeutic effects of PJ34 [N-(6-oxo-5,6-dihydrophenanthridin-2-yl)-N,N-dimethylacetamide.HCl], a selective inhibitor of poly(ADP-ribose) polymerase, in experimental allergic encephalomyelitis are*

associated with immunomodulation. J Pharmacol Exp Ther, 2004. **310**(3): p. 1053-61.
77. Banasik, M., et al., *Specific inhibitors of poly(ADP-ribose) synthetase and mono(ADP-ribosyl)transferase.* J Biol Chem, 1992. **267**(3): p. 1569-75.
78. Veres, B., et al., *Regulation of kinase cascades and transcription factors by a poly(ADP-ribose) polymerase-1 inhibitor, 4-hydroxyquinazoline, in lipopolysaccharide-induced inflammation in mice.* J Pharmacol Exp Ther, 2004. **310**(1): p. 247-55.
79. Marik, C., et al., *Lesion genesis in a subset of patients with multiple sclerosis: a role for innate immunity?* Brain, 2007. **130**(Pt 11): p. 2800-15.
80. Bauer, J., et al., *Astrocytes are a specific immunological target in Rasmussen's encephalitis.* Ann Neurol, 2007. **62**(1): p. 67-80.
81. Zeger, M., et al., *Insulin-like growth factor type 1 receptor signaling in the cells of oligodendrocyte lineage is required for normal in vivo oligodendrocyte development and myelination.* Glia, 2007. **55**(4): p. 400-11.
82. Kajta, M., et al., *Impact of 17beta-estradiol on cytokine-mediated apoptotic effects in primary hippocampal and neocortical cell cultures.* Brain Res, 2006. **1116**(1): p. 64-74.
83. Kipp, M., et al., *Oestrogen and progesterone reduce lipopolysaccharide-induced expression of tumour necrosis factor-alpha and interleukin-18 in midbrain astrocytes.* J Neuroendocrinol, 2007. **19**(10): p. 819-22.
84. McEwen, B.S. and S.E. Alves, *Estrogen actions in the central nervous system.* Endocr Rev, 1999. **20**(3): p. 279-307.
85. Wegmann, T.G., et al., *Bidirectional cytokine interactions in the maternal-fetal relationship: is successful pregnancy a TH2 phenomenon?* Immunol Today, 1993. **14**(7): p. 353-6.
86. Mason, J.L., et al., *Episodic demyelination and subsequent remyelination within the murine central nervous system: changes in axonal calibre.* Neuropathol Appl Neurobiol, 2001. **27**(1): p. 50-8.
87. Lucchinetti, C. and W. Bruck, *The pathology of primary progressive multiple sclerosis.* Mult Scler, 2004. **10 Suppl 1**: p. S23-30.
88. Skripuletz, T., et al., *Cortical demyelination is prominent in the murine cuprizone model and is strain-dependent.* Am J Pathol, 2008. **172**(4): p. 1053-61.
89. Turrin, N.P. and S. Rivest, *Tumor necrosis factor alpha but not interleukin 1 beta mediates neuroprotection in response to acute nitric oxide excitotoxicity.* J Neurosci, 2006. **26**(1): p. 143-51.
90. Kotter, M.R., et al., *Macrophage depletion impairs oligodendrocyte remyelination following lysolecithin-induced demyelination.* Glia, 2001. **35**(3): p. 204-12.
91. Boggs, J.M., *Myelin basic protein: a multifunctional protein.* Cell Mol Life Sci, 2006. **63**(17): p. 1945-61.
92. Moscarello, M.A., F.G. Mastronardi, and D.D. Wood, *The role of citrullinated proteins suggests a novel mechanism in the pathogenesis of multiple sclerosis.* Neurochem Res, 2007. **32**(2): p. 251-6.
93. Aberg, N.D., et al., *Peripheral infusion of insulin-like growth factor-I increases the number of newborn oligodendrocytes in the cerebral cortex of adult hypophysectomized rats.* Endocrinology, 2007. **148**(8): p. 3765-72.

94. Cui, Q.L. and G. Almazan, *IGF-I-induced oligodendrocyte progenitor proliferation requires PI3K/Akt, MEK/ERK, and Src-like tyrosine kinases.* J Neurochem, 2007. **100**(6): p. 1480-93.
95. Darlington, C.L., *Astrocytes as targets for neuroprotective drugs.* Curr Opin Investig Drugs, 2005. **6**(7): p. 700-3.
96. Salmaso, N. and B. Woodside, *Fluctuations in astrocytic basic fibroblast growth factor in the cingulate cortex of cycling, ovariectomized and postpartum animals.* Neuroscience, 2008. **154**(3): p. 932-9.
97. Etgen, A.M., O. Gonzalez-Flores, and B.J. Todd, *The role of insulin-like growth factor-I and growth factor-associated signal transduction pathways in estradiol and progesterone facilitation of female reproductive behaviors.* Front Neuroendocrinol, 2006. **27**(4): p. 363-75.
98. Quesada, A., B.Y. Lee, and P.E. Micevych, *PI3 kinase/Akt activation mediates estrogen and IGF-1 nigral DA neuronal neuroprotection against a unilateral rat model of Parkinson's disease.* Dev Neurobiol, 2008. **68**(5): p. 632-44.
99. Garcia-Segura, L.M., et al., *Estradiol, insulin-like growth factor-I and brain aging.* Psychoneuroendocrinology, 2007. **32 Suppl 1**: p. S57-61.
100. Mendez, P., F. Wandosell, and L.M. Garcia-Segura, *Cross-talk between estrogen receptors and insulin-like growth factor-I receptor in the brain: cellular and molecular mechanisms.* Front Neuroendocrinol, 2006. **27**(4): p. 391-403.
101. Pawlak, J., et al., *Estrogen receptor-alpha is associated with the plasma membrane of astrocytes and coupled to the MAP/Src-kinase pathway.* Glia, 2005. **50**(3): p. 270-5.
102. Irvine, K.A. and W.F. Blakemore, *Remyelination protects axons from demyelination-associated axon degeneration.* Brain, 2008. **131**(Pt 6): p. 1464-77.
103. Naismith, R.T. and A.H. Cross, *Multiple sclerosis and black holes: connecting the pixels.* Arch Neurol, 2005. **62**(11): p. 1666-8.
104. Smith, K.J. and H. Lassmann, *The role of nitric oxide in multiple sclerosis.* Lancet Neurol, 2002. **1**(4): p. 232-41.
105. Lassmann, H., W. Bruck, and C.F. Lucchinetti, *The immunopathology of multiple sclerosis: an overview.* Brain Pathol, 2007. **17**(2): p. 210-8.
106. Hemm, R.D., W.W. Carlton, and J.R. Welser, *Ultrastructural changes of cuprizone encephalopathy in mice.* Toxicol Appl Pharmacol, 1971. **18**(4): p. 869-82.
107. Jurewicz, A., et al., *Tumour necrosis factor-induced death of adult human oligodendrocytes is mediated by apoptosis inducing factor.* Brain, 2005. **128**(Pt 11): p. 2675-88.
108. Lorenzo, H.K. and S.A. Susin, *Mitochondrial effectors in caspase-independent cell death.* FEBS Lett, 2004. **557**(1-3): p. 14-20.
109. Copray, J.C., et al., *p75NTR independent oligodendrocyte death in cuprizone-induced demyelination in C57BL/6 mice.* Neuropathol Appl Neurobiol, 2005. **31**(6): p. 600-9.
110. Ha, H.C., L.D. Hester, and S.H. Snyder, *Poly(ADP-ribose) polymerase-1 dependence of stress-induced transcription factors and associated gene expression in glia.* Proc Natl Acad Sci U S A, 2002. **99**(5): p. 3270-5.

111. Stariha, R.L. and S.U. Kim, *Mitogen-activated protein kinase signalling in oligodendrocytes: a comparison of primary cultures and CG-4.* Int J Dev Neurosci, 2001. **19**(4): p. 427-37.
112. Xia, Z., et al., *Opposing effects of ERK and JNK-p38 MAP kinases on apoptosis.* Science, 1995. **270**(5240): p. 1326-31.
113. Kauppinen, T.M., et al., *Direct phosphorylation and regulation of poly(ADP-ribose) polymerase-1 by extracellular signal-regulated kinases 1/2.* Proc Natl Acad Sci U S A, 2006. **103**(18): p. 7136-41.
114. Tang, D., et al., *ERK activation mediates cell cycle arrest and apoptosis after DNA damage independently of p53.* J Biol Chem, 2002. **277**(15): p. 12710-7.
115. Cohen, R.I., et al., *Nerve growth factor and neurotrophin-3 differentially regulate the proliferation and survival of developing rat brain oligodendrocytes.* J Neurosci, 1996. **16**(20): p. 6433-42.
116. Yoon, S.O., et al., *Competitive signaling between TrkA and p75 nerve growth factor receptors determines cell survival.* J Neurosci, 1998. **18**(9): p. 3273-81.
117. Veres, B., et al., *Decrease of the inflammatory response and induction of the Akt/protein kinase B pathway by poly-(ADP-ribose) polymerase 1 inhibitor in endotoxin-induced septic shock.* Biochem Pharmacol, 2003. **65**(8): p. 1373-82.
118. Pang, Y., et al., *IGF-1 protects oligodendrocyte progenitors against TNFalpha-induced damage by activation of PI3K/Akt and interruption of the mitochondrial apoptotic pathway.* Glia, 2007. **55**(11): p. 1099-107.
119. Barthwal, M.K., et al., *Negative regulation of mixed lineage kinase 3 by protein kinase B/AKT leads to cell survival.* J Biol Chem, 2003. **278**(6): p. 3897-902.
120. Park, H.S., et al., *Akt (protein kinase B) negatively regulates SEK1 by means of protein phosphorylation.* J Biol Chem, 2002. **277**(4): p. 2573-8.
121. Keegan, M., et al., *Relation between humoral pathological changes in multiple sclerosis and response to therapeutic plasma exchange.* Lancet, 2005. **366**(9485): p. 579-82.
122. Panitch, H., et al., *Interferon beta-1b in secondary progressive MS: results from a 3-year controlled study.* Neurology, 2004. **63**(10): p. 1788-95.
123. Group., S.P.E.C.T.o.R.I.-B.-a.i.M.S.S., *Randomized controlled trial of interferon-beta-1a in secondary progressive MS: Clinical results.* Neurology, 2001. **56**(11): p. 1496-504.
124. Cohen, J.A., et al., *Benefit of interferon beta-1a on MSFC progression in secondary progressive MS.* Neurology, 2002. **59**(5): p. 679-87.
125. Wolinsky, J.S., et al., *Glatiramer acetate in primary progressive multiple sclerosis: results of a multinational, multicenter, double-blind, placebo-controlled trial.* Ann Neurol, 2007. **61**(1): p. 14-24.

5 Bibliography

Publications directly related to the thesis:

Articles

P. Acs*, M. Kipp*, C. Beyer, S. Komoly; Estrogen and progesterone treatment prevents cuprizone induced demyelination in C57Bl/6 male mice Glia. 2009 Jun; 57(8):807-14 IF: 4.932 *contributed equally

Sara Veto*, Peter Acs* , Jan Bauer, Hans Lassmann, Zoltan Berente, Gyorgy Setalo, Jr, Gabor Borgulya, Balazs Sumegi, Samuel Komoly, Ferenc Gallyas, Jr and Zsolt Illes: Inhibiting poly(ADP-ribose) polymerase: a potential therapy against oligodendrocyte death Brain, 2010, Volume 133, Number 3, Pp. 822-834 IF: 9.23 *contributed equally

Peter Acs, Samuel Komoly: Selective ultrastructural vulnerability in the cuprizone induced experimental demyelination; submitted for publication

Book chapter

P. Acs, B. Kalman: Pathogenesis of multiple sclerosis: what can we learn from the cuprizone model. In: A. Perl (Ed) Autoimmunity. Humana 2012

Abstracts

Veto S, Acs P, Bauer J, Lassmann H, Berente Z, Sumegi B, Komoly S, Gallyas F Jr, Illes Z, 2010. Inhibiting poly(ADP-ribose) polymerase: a potential therapy against oligodendrocyte death in multiple sclerosis. Clinical Immunology 135: S30-S30

Veto S, Acs P, Bauer J, Lassmann H, Berente Z, Sumegi B, Komoly S, Gallyas F Jr, Illes Z, 2010. Poly(ADP-ribose) polymerase (PARP) is activated in multiple sclerosis pattern III lesions and its inhibition prevents experimental demyelination and oligodendrocyte death. Journal of Neuroimmunology 222:16-16

Veto S, Acs P, Bauer J, Lassmann H, Berente Z, Sumegi B, Komoly S, Gallyas F Jr, Illes Z, 2009. Poly(ADP-ribose) polymerase (PARP) is activated in multiple sclerosis pattern III lesions and its inhibition prevents experimental demyelination and

oligodendrocyte death. Journal of the Neurological Sciences 285: S105-S106 Suppl.

Veto S, Acs P, Bauer J, Lassmann H, Berente Z, Sumegi B, Komoly S, Gallyas F Jr, Illes Z, 2009. Poly(ADP-ribose) polymerase is activated in multiple sclerosis pattern III lesions and its inhibition prevents experimental demyelination and oligodendrocyte death. Multiple Sclerosis 15: S88-S88

Veto S, Acs P, Tapodi A, Lendvai Z, Komoly S, Illes Z, Gallyas F, 2008. Poly(ADP)ribose polymerase inhibitor modifies the activities of various kinase cascades in the cuprizone-induced demyelination model. Multiple Sclerosis 14: S81-S81

Veto S, Acs P, Dolowschiak T, Doppler H, Kanizsai A, Berente Z, ifj Gallyas F, 2007. Cuprizone hatása a mitogén aktiválta protein kináz (MAPK) rendszerekre a corpus callosumban. Folia Hepatologica 11: S40-S40

Veto S, Acs P, Dolowschiak T, Lendvai Z, Gallyas F, Komoly S, Berente Z, 2007. In vivo MRI follow-up of cuprizone-induced CNS changes. Multiple Sclerosis 13: S255-S255

Veto S, Acs P, Berente Z, Szabo A, ifj. Gallyas F, Komoly S, 2006. 4 hydroxiquinazoline hatása a cuprizone indukálta központi idegrendszeri elváltozásokra. Biokémia 30:80-81 S.

Posters

Veto S, Acs P, Bauer J, Lassmann H, Berente Z, Setalo G Jr, Sümegi B, Komoly S, Gallyas F Jr, Illes Z. Poli(ADP-ribóz) polimeráz (PARP) gátlás: az oligodendrocyta pusztulás és a demyelinisatio potenciális terápiája.
Magyar Immunológiai Társaság 39. Vándorgyűlése, November 3-5, 2010, Szeged, Hungary

Veto S, Acs P, Bauer J, Lassmann H, Berente Z, Setalo G Jr, Sumegi B, Komoly S, Gallyas F Jr, Illes Z. Inhibiting poly(ADP-ribose) polymerase (PARP): a potential

therapy against oligodendrocyte death and demyelination in multiple sclerosis.
14th Congress of the Europian Federation of Neurological Societies, September 25-28, 2010, Geneva, Switzerland

Veto S, Acs P, J. Bauer J, H. Lassmann, Z. Berente, B. Sumegi, S. Komoly, F. Gallyas Jr, Z. Illes. Poly(ADP-ribose) polymerase is activated in multiple sclerosis pattern III lesions and its inhibition prevents experimental demyelination and oligodendrocyte death.
25th Congress of the European Committee for Treatment and Reasearch in Multiple Sclerosis, September 9-12, 2009, Düsseldorf, Germany

Veto S, Acs P, Berente Z, Doppler H, Kanizsai A, Lendvai Z, Komoly S, Illes Z, Gallyas F Jr. Inhibition of poly(ADP)ribose polymerase protects against cuprizone induced demyelination by preserving mitochondrial integrity in a degenerative murine model of multiple sclerosis.
12th Meeting of the Hungarian Neuroscience Society, 22-24 January, 2009, Budapest, Hungary

Veto S, Acs P, Tapodi A, Lendvai Z, Komoly S, Illes Z, Gallyas F Jr. Poly(ADP)ribose polymerase inhibitor modifies the activities of various kinase cascades in the cuprizone induced demyelination model.
World Congress on Treatment and Research in Multiple Sclerosis. September 17-20, 2008, Montreal, Canada

Veto S, Acs P, Dolowschiak T, Lendvai Z, Gallyas F Jr., Komoly S, Berente Z. In vivo MRI follow-up of cuprizone induced CNS changes.
23rd Congress of the European Committee for Treatment and Research of Multiple Sclerosis (ECTRIMS) and the 12th Conference of Rehabilitation in Multiple Sclerosis (RIMS), October 11–14, 2007, Prague, Czech Republic

Veto S, Dolowschiak T, Kanizsai A, Doppler H, Acs P, ifj. Gallyas F, Komoly S,

Berente Z. Cuprizone indukálta központi idegrendszeri elváltozások *in vivo* követése MRI segítségével.
37. Membrán-Transzport Konferencia, May 22-25, 2007, Sümeg, Hungary

Veto S, Acs P, Berente Z, Szabo A, ifj. Gallyas F, Komoly S. 4-hydroxiquinazoline hatása a cuprizone indukálta központi idegrendszeri elváltozásokra.
A Magyar Biokémiai Egyesület 2006. évi Vándorgyűlése, August 30 – September 2, 2006, Pécs, Hungary

Presentations

Cuprizone induced demyelination – a novel model for multiple sclerosis
requested speech, 2008, NIH, NCI, Laboratory of Molecular Biology

Toxin induced demyelination in the central nervous system
requested speech, 2010, FDA, Laboratory of Immunology

Oligodendrocyte apoptosis and primary demyelination in the cuprizone induced experimental demyelination
requested presentation, 2011, UT Southwestern Medical Center

Publications not connected to the thesis

Kovács GG, Kurucz I, Budka H, Adori C, Müller F, Acs P, Klöppel S, Schätzl HM, Mayer RJ, László L. Prominent stress response of Purkinje cells in Creutzfeldt-Jakob disease. Neurobiol Dis. 2001 Oct;8 (5):881-9.

6 Acknowledgement

I generously and gratefully thank to my mentor, teacher and project leader, Prof. Samuel Komoly M.D., Ph.D., D.Sc. for his leadership, support, advices and for providing me the opportunity to perform this project.
I am grateful to Prof. Zsolt Illes M.D., Ph.D., D.Sc for his excellent contribution and support in the studies.
I wish to thank to Prof. Ferenc Gallyas Jr M.D., Ph.D, D.Sc. and to Sara Veto M.D., Ph.D. for the fruitful collaboration throughout the whole study.
I owe special thanks to Hans Lassmann and the Centre for Brain Research, Medical University of Vienna for the flourishing collaboration.
I appreciate the collaboration and great support of Univ.-Prof. Dr. hum. biol. Cordian Beyer and Markus Kipp M.D., Ph.D at the University Hospital Aachen, Institute of Neuroanatomy.
I am grateful to Prof. Gallyas Ferenc Sen for his technical support and advices.
I thank to Maria Mazlo M.D., Prof. Laszlo Seress M.D. Ph.D., D.Sc. and Hajnalka Abraham M.D., Ph.D. for their help.
I cordially acknowledge the help of Krisztina Fulop, Adam Feldmann and Erno Bognar.
I am grateful to my family for their support and unconditional love.